# PLASMA NITRIDING BEHAVIOR OF AISI 316 L STAINLESS STEEL

A Thesis Submitted to the
Graduate School of Natural and Applied Sciences of
Dokuz Eylül University
In Partial Fulfillment of the Requirements for
the Master of Sciences in Mechanical Engineering,
Mechanics Program

by

Hakan GÜNAY





August, 1999
İZMİR

M.Sc. THESIS EXAMINATION RESULT FORM

We certify that we have read this thesis and that in our opinion it is fully adequate, in scope and in quality, as a thesis for the degree of Master of Science.

Prof. Dr. Süleyman Karadeniz

(Advisor)

Prof.Dr. Sami AKSOY

(Committee Member)

Prof.Dr. Tevfik AKSOY

(Committee Member)

Approved for the

Graduate School of Natural and Applied Sciences

Prof.Dr.Cahit Helvacı

Director

Graduate School of Natural and Applied Sciences

# ACKNOWLEDGEMENTS

I am gratefully acknowledge the support and encouragement given by Süleyman Karadeniz during the course of the investigation.

I am really indebted to Serdar Karaoğlu for supplying valuable documents and for his great helps.

I am grateful to Faik Soysal for his helpful suggestions and assistance in carrying out the experiments. I am also grateful to Ahmet Yiğit for specimen preparation and other production work.

During the thesis, assistance from these friends is also appreciated: Zafer Azem, İsmail Özdemir and Hasan Öztürk .

Finally, I thank my parents and my brother not only for their great help but also encouragement and patience that supported me throughout the study.

**Hakan GÜNAY**

# ABSTRACT

In this investigation, the surface hardening of AISI 316L stainless steel, an important engineering material, by using plasma nitriding technique has been aimed with various temperatures (400...600°C), times (1...10h) and the volumetric ratio of $N_2$ in the plasma atmosphere of $N_2$+$H_2$ gaseous mixture as process parameters.

Microhardness measurements and optical microscopy techniques have been used to investigate the nitriding response of the steel. The work has focused on the surface hardening behavior of the steel, the morphology of the nitrided layers and study of wear properties of plasma nitrided specimens. Pin-on ring type of wear tests were carried out under dry sliding conditions.

Besides its reduced processing times, causing no environmental pollution, considerably smooth surfaces, low electricity and gaseous consumptions and compatibility for automation, the plasma nitriding process with controllable diffusion thickness and hard but less ductile metallic surfaces, has allowed for remarkable increase in the hardness of AISI 316L stainless steel.

By microhardness measurements and optical microscope investigations, the maximum surface hardness and the deepest diffusion layer has been obtained in the plasma nitrided sample over a period of 7h 550°C in a nitriding atmosphere containing %40$N_2$+%60$H_2$ gaseous mixture.

The case depth were found to increase with increasing process temperature and time. Nitrogen content of the plasma nitriding atmosphere while increasing slightly decreased the case depth and surface hardness.

Wear rates were observed to increase with increasing compound layer thickness and decreasing surface hardness.

# ÖZET

Önemli bir mühendislik malzemesi olan AISI 316L paslanmaz çeliğinin plazma nitrürasyonu yöntemi kullanılarak sertleştirilmesi amaçlanan bu çalışmamızda işlem parametreleri olarak sıcaklık (400...600°C), zaman (1...10h) ve $N_2$+$H_2$ karışımından oluşan plazma atmosferindeki azot gazının hacimsel oranı alındı.

Çeliğin nitrürasyon işlemine cevabını araştırmak için mikrosertlik ölçümleri ve optik mikroskobi teknikleri kullanıldı. Çalışma; çeliğin yüzey sertleşme davranışı, nitrürlenmiş tabakaların şekli ve plazma nitrürlenmiş numunelerin aşınma özelliklerinin araştırılmasında yoğunlaştı. Pim-halka tipi aşınma testleri kuru sürtünme şartlarında gerçekleştirildi.

İşlem sürelerinin kısalığı, çevre kirliliğine neden olmaması, işlem neticesinde yüzeyde çok az pürüzlülüğün oluşması, düşük elektrik ve gaz sarfiyatı ve otomasyona elverişliliğinin yanısıra difüzyon tabakası kalınlığının kontrolüne ve sert fakat daha az gevrek metal yüzeyleri elde edilebilmesine imkan sağlayan plazma nitrürasyonu yöntemiyle AISI 316L paslanmaz çeliğinin sertliğinde önemli artışlar kaydedilmiştir.

Yapılan mikrosertlik ölçümlerinin ve optik mikroskop gözlemlerinin ışığında en fazla yüzey sertliğinin ve en derin difüzyon tabakasının 7 saat 550°C 'de %40$N_2$+%60$H_2$ gaz karışımı kullanıldığı durumda oluştuğu gösterilmiştir.

Difüzyon tabakası kalınlığı artan işlem süresi ve sıcaklığı ile artmaktadır. Azot yüzdesinin artması ile difüzyon tabakası kalınlığında ve yüzey sertliğinde bir azalma meydana gelmektedir.

Aşınma miktarının, artan kompond tabaka kalınlığı ve azalan yüzey sertliği ile arttığı görülmüştür.

# CONTENTS

Page

Page

Chapter Three
PROPERTIES OF STAINLESS STEEL



Chapter Four
EXPERIMENTAL STUDIES



Chapter Five
RESULTS AND DISCUSSION



Chapter Six
CONCLUSIONS

# LIST OF TABLES

Page

# LIST OF FIGURES

Page

Page

# CHAPTER ONE
# INTRODUCTION

## 1.1 Introduction

Among the thermochemical processes for the improvement of surface properties of machine components, nitriding holds an important position in industry today. Together with conventional gas and salth bath nitriding there is a new process called plasma nitriding or ion-nitriding, which is using the glow discharge technology to generate nitrogen ions to the surface of a metallic part for diffusion, has been developed to complete industrial application in the last few decades.

Because of its special basic technique -making use of the plasma of a glow discharge- plasma nitriding has a large variety of properties to offer and therefore opens up new perspectives in the field of nitriding.

The plasma nitriding of steels is here the oldest plasma assisted process in industrial use. In case of conventional thermochemical processes the workpiece has to be treated at the temperature which is necessary for thermal activation of precursor (powders, paste, salt baths, gas etc.) in order to get diffusible, layer forming species at the workpiece surface. The workpieces to be treated are placed in a vacuum chamber electrically insulated against the wall of the vessel.

This process is done in a vacuum furnace at low temperatures (400...600°C) and can be applied to any ferrous metal. Today, plasma nitriding is used on a large scale in industries concerned with iron, steel, cast iron, titanium and sintered iron products.

The principle of a current-carrying substance between an anode and cathode is known from the galvanic plating process. The plasma nitriding process is carried out in a nitrogen-hydrogen gas mixture at 1 to 10 Torr pressure. By means of a high d.c. voltage (500-1000V), the gas is excited and ionized. Because of the glow involved with the excited gas state (plasma), the phenomenon is also called a glow discharge.

The positive nitrogen ions, which are produced inside the glow discharge, are attracted toward the negatively connected workpieces; they hit upon the surfaces, are thus occluded, and heat up the pieces to the necessary diffusion temperature, so it does not own any classical heating devices. This means plasma nitriding furnace is purely a container with the purpose of holding a technical vacuum inside and serving as the anode for the glow discharge.

After plasma nitriding, the surface layers have essentially the same macroscopic structure as conventionally nitrided surfaces. There are, however, considerable differences with regard to macroscopic details. The compound layer at the surface, which consists of an intermetallic compound of iron plus nitrogen ($\gamma'$ and $\varepsilon$), is rich in nitrogen and only a few micrometers in thickness. The diffusion layer is underneath the compound layer. Its hardness depends mainly upon the amount of alloying elements in the steels. Layer structure as well as layer properties can be properly adjusted depending on the demand of the users, since a large variety of process parameters is available for the treatment.

As diffusion elements N and C are mainly used, either separately or mixed, scarcely B, Ti, Si, and Cr. By plasma nitriding today nearly all ferrous metals (low and high alloyed steels), powder metals and nonferrous metals (Ti, Al, Mo, W, etc.) can be treated for enhencing wear and corrosion resistance as well as the fatigue strength.

Plasma nitriding has proven to extend the life of tooling and machinery components used in the metal forming, plastics, forging and die casting industries up to 10 times, depending on application.

## 1.2 Literature Review

The concept and principles of the plasma nitriding process were first established in Germany by Bernard Berghaus in the early 1930's (Berghaus,1932). The following work was concerned with the establishment and control of glow discharges from high currents (Berghaus,1939; Berghaus,1956; Berghaus,1961).

Ionen, a private company owned by Berghaus in Cologne-Germany was responsible for the industrial exploitation of the technology generated. Following the death of Berghaus in 1965, Klockner Ionen was formed in 1967 and thus gained access to this technology which formed the basis of the international commercialization of this technique (Hombeck & Bell,1991). Plasma nitriding installations of various sizes have been available from the Klockner Ionen GmbH, Cologne, Germany since 1972 (Edenhofer,1976). Today, industrial installations operate in many countries, and heat treatment corporations having plasma nitriding units can be visited in Internet web sites.

One of the other new company who works in the plasma nitriding business is called Plateg, "Plasma Technik Grün GmbH", was founded in 1986. Plateg has since been a leading company in the advance of plasma technology and has given many impulses to promote the use of advanced technology when treating metal surfaces. Their complete fields of activity are especially for plasma nitriding and coatings by means of plasma CVD (Chemical Vapour Deposition) and PVD (Physical Vapour Deposition) as well as for cleaning and degreasing of metal surfaces. Also they work in the field of coatings for the resistance of wear and corrosion. They can be treated parts of up to a length of 3 m or a diameter of up to 1m. In fact there are some big companies have a furnace of 10m length and a diameter of up to 4m in some parts of the U.S.A.

The results of studies on the physical aspects or mechanism of the process are quite conflicting. No consensus has been reached about a proper model of the process so far (Li & Manory, 1996). The Kölbel (Kölbel, 1965) and Hudis (Hudis, 1973)

models in particular are very well known, but the mechanism of nitriding described in each of them is totally different. In Kölbel's model elemental iron is sputtered from the cathode workpiece by nitrogen ions and highly energized neutral particles. These iron atoms form FeN in the plasma which is deposited on the workpiece surface. Since FeN is not a thermally stable compound, it degrades to iron nitrides with a lower nitrogen content, producing nitrogen atoms that are capable of diffusion. The continuous diffusion of the nitrogen atoms into the material's surface forms the required case. Based on mass spectrometry results, Hudis (Hudis, 1973) suggests that nitrogen mass transfer during plasma nitriding is predominantly due to bombardment of the workpiece by plasma species containing nitrogen. Another study on the mechanism of the process (Tibbets,1974) pointed out the adsorption of neutral atomic nitrogen to be the cause of nitriding.

Normally, specimens in plasma nitriding process are in cathode position and they are heated to the process temperature by the ion bombardment. But in the case of samples at the anode position radiation heating (Zlatonovic, Kunosic & Tomcik, 1986), or resistance heating (Michalski, 1993) can be applied. In the former study, Zlatonovic et al. explained the process by the direct diffusion of the active species from the cathode to the anode. In the other investigation, Michalski studied Armco iron plasma nitrided in various glow discharge regions, i.e. on the cathode, on the anode, and on a substrate isolated from the cathode and anode (at plasma potential). He saw that the nitriding process would occur in regions other than the cathodic region if the substrate is hot enough. He examined the differences in the growth kinetics and surface morphology of the nitrided layers, depending on the region where nitriding process took place. It has been concluded that, sputtering effect is not necessary for glow discharge nitriding and atomic nitrogen can be chemi-sorbed on the hot surface and diffuse deep into the substrate.

After the first laboratory experiments and patents, many plasma nitriding studies have been conducted primarily dealing with the metallurgical aspects, i.e. the influence of the plasma nitriding treatment on the different materials, the production of different

layers and the examination of their properties. For example, some companies are conducted one of the new plasma nitriding process called Pulse Plasma Technology successfully for metal surface treatment and also some of them experienced by plasma etching for the production of microprocessors.

İnal and Robino (İnal & Robino, 1982; Robino & İnal, 1983) researched the structures of plasma nitrided low alloy commercial steels using field ion microscopy (FIM) and transmission electron microscopy (TEM) techniques, and the relationship between nitriding parameters and hardenability characteristics of the steels. These studies showed that, the nucleation and growth of very small nitride precipitates adjacent to the carbides were already present following tempering. This was seen as an indication of the dissolution of the carbides during the process, although some of the carbides were still undissolved following 10h of plasma nitriding at 520°C.

The outermost layer, compound layer or white layer, of the plasma nitrided materials has been the subject of many studies. Investigations related to structure, composition and thickness of the compound layer have been carried out using X-ray diffraction (XRD), Transmission Electron Microscopy (TEM), Electron Probe Micro Analysis (EPMA), Optical Microscopy and Scanning Electron Microscopy (SEM) techniques.

Kurny, Mallya and Mohan Rao (Kurny, Mallya & Mohan Rao, 1986) investigated the nature of the compound layer formed on a plasma nitrided low alloy steel (En40B) by the XRD technique and optical metallography. They reported that the structure of the compound layer gradually transforms from a predominantly ε nitride to a predominantly γ′ nitride structure with increasing treatment time. They also observed that the thickness of the compound layer produced after about 5h of treatment, decreases with further increase in time.

Chyou and Shih (Chyou & Shih, 1990) investigated the structure and electrochemical properties of a plasma nitrided low alloy steel (AISI 4140). They observed that $\gamma'$ forms at greater depths than $\varepsilon$.

Based on a TEM study (Xu, Wang, Yu & Hei, 1996) it was concluded that; the compound layer consists of columnar $\varepsilon$ and $\gamma'$, the former precipitating thin $\gamma'$ phases in some orientations, and supersaturating nitrogen atoms produces lattice distortion in the columnar $\gamma'$.

Çelik and Karadeniz (Çelik & Karadeniz, 1996) investigated the structure and composition of compound layer formed on a low alloy steel (AISI 4140) plasma nitrided at various process conditions. They observed a decrease in the thickness of the compound layer at higher treatment temperatures and longer treatment times.

Recently, some investigations (Haruman, Bell & Sun, 1992; Lampe, Eisenberg & Laudien, 1993; Li & Manory, 1996) on the phenomenon of pore formation on the top surface of compound layer have appeared.

Plasma nitriding has been gradually incorporated in many industrial applications particularly during the last 25 years. Workers in plasma nitriding have explored the possibilities of this technique almost in every type of steel. Besides studies on low alloy steels, some examples of which given above, there have been many investigations concerning plasma nitriding behavior of high alloy steels (Cohen, Boas & Rosen, 1986; Özbaysal, İnal & Romig, 1986; Takada, Ohizumi, Miyamura, Kuwahara, Kikuchi & Tamura, 1986; Miyamura, Takada, Kuwahara & Kikuchi, 1986; Sato, Takahashi, Inoue, Yamazaki & Nitoh, 1988; Albarran, Juarez-Islas & Martinez, 1992; Kuppasami, Terrance, Sundararaman & Raghunathan, 1993; Kuppasami, Sundararaman & Raghunathan, 1993).

The wear mechanism of plasma nitriding steels is not fully understood, even though it has been extensively studied.

Bell and Sun (Bell & Sun, 1990) showed that a thick and strong nitrided case is required for plasma nitrided specimens to bear high loads without severe wear. In another study (Karamış,1991) on the same low alloy steel (En40B) with similar process conditions a combination of higher hardness and deeper case has been advised for reducing the extent of material loss under dry and abrasive-containing lubricated conditions. It was surprisingly observed that some samples having a thicker compound layer wear less than others under dry conditions.

It has been experimentally demonstrated by e.g. Sun and Bell (Sun & Bell, 1991), and Karamış (Karamış,1992; Karamış, 1993) that a poly-phased and thick compound layer, which is extremely brittle, increases the wear rate of the materials especially at the initial stage of the wear process. But this is not a general rule and there are several examples (e.g. Karamış,1991) of contradicting behavior.

Peng (Peng, 1989) investigated the abrasive wear behavior of a hot work die steel subjected to a range of surface treatments such as nitrocarburising, plasma nitriding and spark discharge cladding. He concluded that modified surfaces possess improved resistance to abrasive wear, and plasma nitrided surfaces has the highest relative wear resistance.

The wear behavior of plasma nitrided martensitic stainless steel, AISI 440C, has been investigated under various contact conditions (Sun, Bell & Wood, 1994) and it was observed that the short time nitrided layers exhibited better wear resistance than the long time nitrided layers produced at similar temperatures.

### 1.3 Aim Of The Study

The aim of this study is to investigate the plasma nitriding behavior on the chosen test material (austenitic AISI 316 L Stainless Steel), which is used as a biomaterial extensively. Most of the work has focused on; the surface hardening behavior of this steel, the morphology of the nitrided layers, and study of wear properties of plasma nitrided specimens.

To carry out a comparative study, first, specimens were prepared and plasma nitrided for various parameters such as time, temperature and gas composition. Then, microhardness measurements were utilized to obtain the hardness profiles of plasma nitrided samples. Finally, pin-on-ring type of wear tests were carried out to determine effect of plasma nitriding process on the wear performance of the specimens.

From the analysis of the results, some correlations between process parameters and mechanical properties of the specimens were examined.

# CHAPTER TWO
# PLASMA NITRIDING

## 2.1 The Principle of Plasma Nitriding

### 2.1.1 Equipment and Process Data

In order to get a better understanding of the glow discharge technique used in plasma nitriding and of the processes involved, we must first consider the plasma nitriding equipment (Fig.2.1). Its main elements are the vacuum furnace, the gas distribution system and the electric unit.

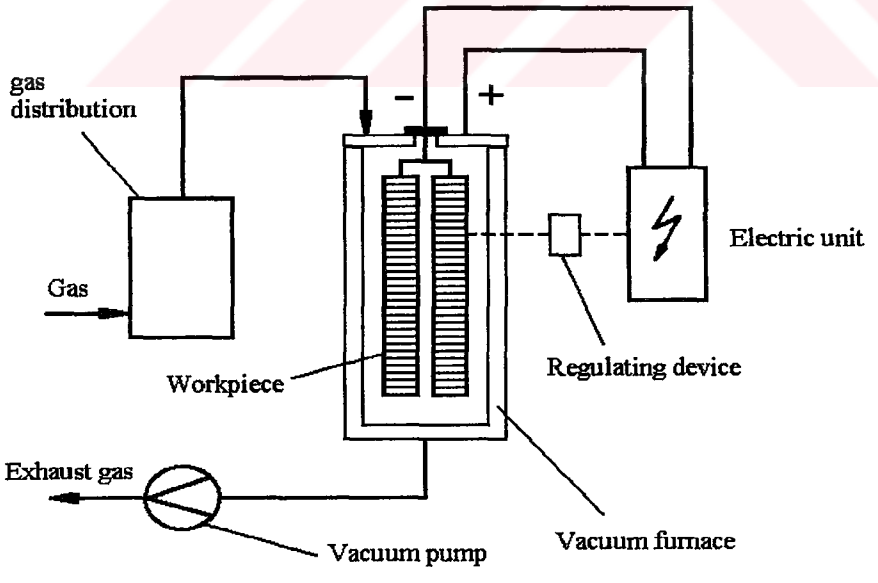


**Figure 2.1 Plasma nitriding equipment**

The components to be plasma nitrided are electrically isolated and suspended or placed in the vacuum furnace. Together with the vacuum pump, the gas distribution system enables the furnace to be evacuated, filled with the appropriate treatment gas and maintained at the required vacuum, usually between 13.3 to1333 Pa (0.1 to 10 torr). A d.c. voltage which can be set any value from about 100 volts to approximately 1500 volts, is applied between the cathode on which the workpiece to be plasma nitrided is placed and the anode which is usually connected to the wall of the furnace. Under this potential difference, the molecules and atoms of the treatment gas are excited and ionized, producing the typical luminous phenomenon known as glow discharge. The positive ions of the treatment gas are accelerated towards the negatively connected component and hit its surface with tremendous kinetic energy. The release of this energy heats the workpiece up and the ions are occluded into its surface. Thus, the furnace does not require a separate heating system.

The electric units are equipped with current and voltage control elements as well as a high speed breaker system to control unstable discharge phenomena.

Plasma nitriding can be carried out using either pure nitrogen or mixtures of nitrogen with hydrogen. Gas consumption during processing is very modest due to the low pressure employed.

The temperature of the workpiece is measured with the aid of thermocouples and regulated by means of a controller varying the power output of the electric unit. The treatment temperature is, in most cases, set between 400 and 600 °C , depending on the composition and structure of the material to be treated as well as the stress which the workpiece will have to resist. A particular advantage of plasma nitriding is the fact that even at low temperatures of between 350 and 450 °C nitrogen saturation of the surface is possible.

Typical treatment times vary from 1 hour to 20 hours, depending on the grade of steel and the required depth of hardening. But some investigations employing

treatment times as long as 100 hours have appeared in the literature (Karamış,1991; Karamış, 1992; Karamış, 1993; Sun, Bell & Wood, 1994)

### 2.1.2 Technique and Control of the Glow Discharge

A glow discharge is produced by the shock excitation of gas atoms and molecules in an electric field in accordance with physical laws. The prerequisites of the appearance of a glow discharge are the presence of a low pressure gas (medium-high vacuum) and the application of a voltage of about 300 V minimum depending upon the gas pressure between two electrodes in the discharge vessel. Fig.2.2 shows the voltage-current characteristics of different types of discharge. The regions A-B (range of the Geiger-counter tube), B-C (Townsend discharge), etc., where the current is extremely low, are of no interest here. The normal glow discharges used in industry (glow lamps, fluorescent tubes, etc.) are maintained with relatively low energies and weak currents, i.e. they work in the region of normal stable and low current glow discharge (E-F). Plasma nitriding processes, however, are associated with high current and power densities and occur in the region of the abnormal, unstable and current-intensive glow discharge. The command and control of this unstable, abnormal glow discharge is the most essential feature in the production of truly plasma nitrided surface layers. The characteristics of this type of discharge clearly indicate that quite a few problems are involved in such control. When working in this abnormal region of the glow discharge (just in front of point G) a slight, localized increase in current density would quickly result in a concentration of the discharge at that particular point.

The possibility that the abnormal, unstable glow discharge may turn into the stable arc discharge has long been a serious obstacle to the large-scale application of plasma nitriding in industry. It was a major achievement of Bernhard Berghaus to realize these problems at an early stage and to have solved them subsequently by systematic developments (Edenhofer, 1974a).

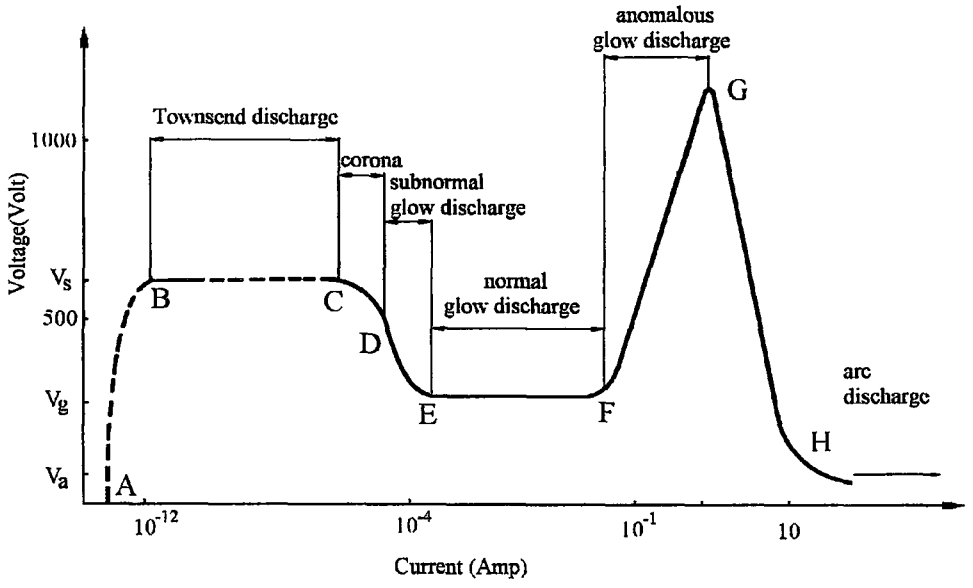


**Figure 2.2 Voltage-current characteristics of different types of discharge**

Nowadays, modern electronic high-speed breaker systems are able to interrogate the current and voltage variations about a thousand times per second and interrupt the discharge for very short periods even if only slight changes are detected. These systems prevent the formation of arcs so that the glow discharge can be safely maintained at high current densities in the extremely abnormal region.

## 2.2 The Plasma State

A variety of nitrogen-providing media are used in nitriding. In accordance with the well known states of matter, nitriding may be classified as solid nitriding, liquid nitriding or gas nitriding. In addition to these three states of matter, there is a further, much more active condition sometimes described as fourth state of matter: the plasma state. As the name infers "plasma nitriding" uses this plasma state.

### 2.2.1 Generation of the plasma

A plasma consists of electrically charged particles, i.e. ions and electrons. In other words, the plasma state is reached by ionizing gas atoms or molecules. In a purely thermal process, this state can only be reached by heating gas to a temperature of at least some hundred thousand degrees. If, however, electricity is employed, this state can be easily reached as in the glow discharge. The small number of charge carriers which are present in any gas are accelerated in the voltage drop between cathode and anode. Collision processes involving other gas particles will dissociate molecules of the treatment gas as well as excite and ionize atoms and molecules. New charge carriers are thus continuously produced; the electrons being accelerated towards the anodically-connected wall of the furnace and the positive ions towards the cathodically-connected workpiece.

The voltage applied does not drop in a linear way between the wall of the furnace and the workpiece, such as it would in an extremely high vacuum, but is greatly modified by the positive space charge which builds up in front of the workpiece. Accordingly, almost the entire applied voltage drops only a few millimeters in front of the cathode (see the upper part of Fig.2.4). This is why the voltage drop is called "cathode fall". All the collision and ionization processes which are an essential feature of this type of surface treatment take place within the region of the cathode fall. Thus, the perfect plasma state of the treatment gas is only produced immediately in front of the workpiece surface (within the cathode fall region), while the remaining treatment space in the vacuum furnace is filled with normal treatment gas which is somewhat enriched in charge carriers. The positive space charge has the effect of a projecting anode so that surface treatment in the plasma of the glow discharge is practically independent of the distance between the workpiece and the wall of the furnace.

The cathodic luminous phenomena called "glow seam" is also limited to a narrow space around the workpiece as can be seen in Fig.2.3. This figure shows the interior

of the plasma nitriding vacuum chamber, used in this study, charged with various workpieces. The glow seam follows each individual contour of the workpieces so that all surfaces, including notches and bores, are submitted to uniform ion bombardment, creating a uniform hardness.

**Figure 2.3 Workpieces surrounded by a glow seam**

### 2.2.2 The reaction of the plasma with the surface of the workpiece

In the cathode fall, the positive nitrogen ions produced by collision processes are strongly accelerated towards the surface of the workpiece. Depending on the voltage applied and the number of particles available, kinetic energies ranging from a few, to several hundred electron volts are produced in this process. These values correspond to atomic plasma temperatures of about ten thousand to several hundred thousand degrees.

After having traversed the applied voltage, these "hot" i.e. high-energy, ions hit the workpiece surface with a certain kinetic energy ($E_{ion}$). This may give rise to the following processes:

*1) Sputtering*

When the ions hit the surface of the workpiece, metal atoms (Fe as well as alloy constituents such as Cr, Mo, Al, W, etc.) are detached (Fig.2.4). Sputtering may be considered a vaporization process the very "hot" ion hitting the surface will intensely heat a localized surface area of the workpiece causing atoms in that particular region to vaporize. These localized temperatures of several thousand degrees are limited to extremely small surface areas and do not harm the workpiece. The average temperature of the surface corresponds exactly to the workpiece temperature, as it was preset, in accordance with the required treatment. This can be proved by measuring the temperatures with the aid of thermocouples or radiation pyrometers.

During this sputtering process, part of the ion energy is converted into work (A) to detach atoms and electrons from the surface, and into kinetic energy ($E_{kin}$) of the detached particles.

$$E_{ion} = A+E_{kin}$$

As well as metals, non metallic elements such as carbon, oxygen, nitrogen, etc. are also detached (Fig.2.4). In this way the surface can be freed from carbides, oxides, etc. Due to the secondary diffusion of these elements (preferably along the grain boundaries) to the surface, the sputtering process has a profound effect upon their concentration and behavior even inside the material.

As far as oxygen is concerned, sputtering results in a unique surface depassivation. This applies also to the strongly adherent oxide layers found on high chromium and stainless steels.

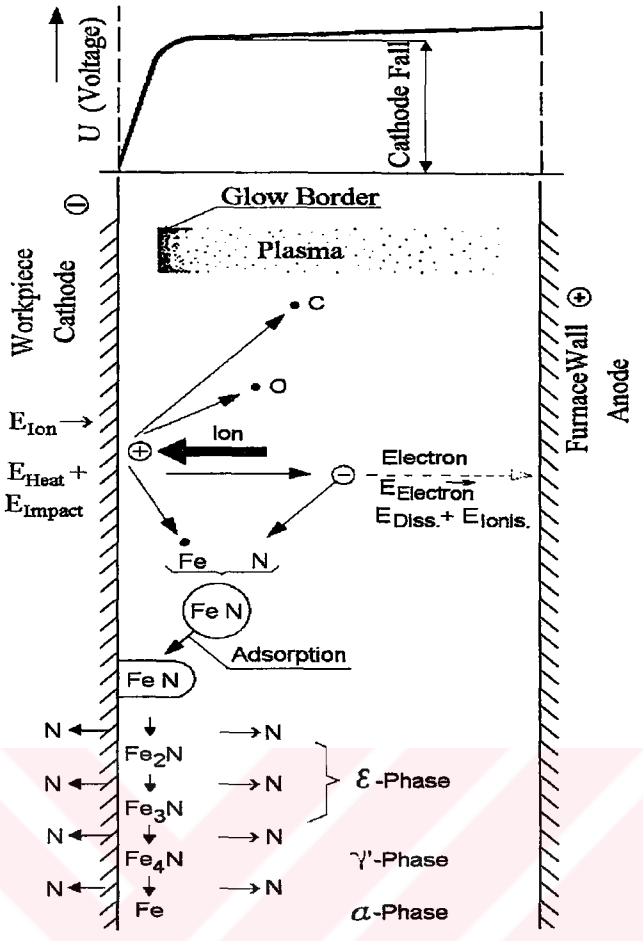


**Figure 2.4 Surface reactions during plasma nitriding**

*2) **Heating***

When the nitrogen ions hit and penetrate the topmost atom layers of the workpiece surface, the remaining ion energy is converted into heat (Q) to heat the workpiece. Thus the workpieces to be treated do not require any external heating. The following equation of the energy balance results:

$$E_{ion} \Rightarrow A + E_{kin} + Q$$

If gas mixtures are used instead of pure nitrogen, ions of other elements such as hydrogen, carbon, oxygen, etc. will also be able to penetrate and heat the workpiece.

*3) Condensation*

It is only to an extremely small extent that the transfer of nitrogen from the plasma into the surface of the workpiece is caused by direct occlusion of ions into the iron lattice (ion bombardment). The most important factor dominating the nitrogen absorption is associated with the sputtering process referred to above. Iron atoms which are detached from the surface can combine with the highly reactive nitrogen atoms in the plasma near the surface of the workpiece and will then, owing to adsorption, be deposited as iron nitride (FeN) on the workpiece surface (Kölbel, 1965). Thus an appositely directed condensation process is superimposed on the sputtering effect.

The iron nitride (FeN) produced in the plasma, having a theoretical nitrogen content of 25.05 per cent by weight, can be condensed on a constantly-cooled surface where, with suitably intensive cooling, the majority of it can be preserved. Investigations of such condensation processes have indicated that the nitride FeN is actually produced during plasma nitriding. Up to 19.7% of nitrogen could be found by chemical analysis of the condensate. The FeN nitride which is condensed on uncooled cathodic workpiece surfaces (i.e. 400 to 600 °C depending on the plasma nitriding temperature) is unstable and decomposes into the lower nitrides $Fe_2N$, $Fe_3N$, and $Fe_4N$ (Fig.2.4) (Kölbel, 1965). The nitrogen which is liberated in this process will diffuse into the workpiece and, in part , back into the plasma.

The two processes sputtering and condensation, depend to a great extent on the type of gas used (ammonia, nitrogen, hydrocarbon, etc.). Furthermore, their mutual relationship can be influenced by varying other treatment parameters such as the pressure and voltage.

If for example, the gas pressure is set to a lower value (reduced particle density), there are longer free paths with a smaller probability collision. The detached atoms can thus move a greater distance away from the workpiece surface, i.e. the possibility

of back-diffusion is reduced. Such a parameter setting is of importance in depassivation processes in connection with the removal of oxide layers.

If the gas pressure in the furnace is higher, there is increased back-diffusion. The gas pressure setting can therefore be used to control the thickness of the compound zone.

The material transfer and the resulting increase or decrease in the weight of the workpiece is mainly controlled by the two counteracting processes of sputtering and condensation. Positive and negative changes in weight as well as extremely precise dimensional control can thus be obtained by varying the intensity of these two processes.

## 2.3 The Diffusion of Nitrogen

Investigations into the kinetics of nitriding have been made since the introduction of the process and continue today. In particular, attempts have been made again and again to reduce the extremely long treatment times associated with conventional gas nitriding by accelerating the process of nitrogen occlusion. The first laboratory tests of the plasma nitriding process showed that, as compared to gas nitriding, plasma nitriding considerably reduced the time of nitrogen occlusion.

Although this accelerated hardening effect in plasma nitriding has not been of primary importance in the large scale industrial application of the process, the decisive factors being the precisely controllable structure of plasma nitrided components and their resulting special properties, it is important, from a metallurgical point of view, to know which factors cause the accelerated nitrogen diffusion.

The explanation given in previous years - depassivation of the surface due to cathode sputtering and increased gas activity - were bound to remain inconclusive as long as the kinetics of the formation of plasma nitrided layers were unknown.

It was not until the nitrogen occlusion in plasma nitriding was found to be mainly caused by the iron sputtering and the subsequent iron nitride (FeN) condensation on the surface (Kölbel, 1965), that a reasonable explanation of the accelerated diffusion in plasma nitriding could be given.

Thus at the very outset of the plasma nitriding process, the nitrogen-rich phase (FeN) is condensed on the workpiece surface -its immediate disintegration liberates nitrogen which diffuses into the workpiece. In gas nitriding, the surface concentration of nitrogen is established gradually, first a solid solution in ferrite (α-iron) and then conversion to nitrides with increasing nitrogen content- $Fe_4N$, $Fe_{3-2}N$. The abundant supply of nitrogen in plasma nitriding results in a very fast nitrogen saturation of the α-iron so that, only a few minutes later, coherent layers of iron nitrides exist in equilibrium with the saturated iron. For precisely the same reason, plasma nitriding at extremely low temperatures e.g. 350°C, can produce compact coherent iron nitride layers after only a few hours.

The FeN iron nitride which is condensed on the surface and the resulting high surface concentration of nitrogen yield a concentration gradient which is very steep at the beginning. Experimental results show that it is only after treatment times of ten hours and more that the nitrogen penetration in plasma nitriding no longer progresses at a faster rate in gas nitriding.

On the basis of these results it becomes obvious that the increased concentration gradient alone cannot account for the accelerated diffusion observed. With the build-up of coherent iron nitride phases in gas nitriding, (after about 1 to 2 hours) the concentration gradients in the two processes become similar, since the saturation concentration of the α-iron is reached.

The other important factor with regard to the depth of nitrogen penetration, the temperature dependent rate of diffusion of nitrogen in iron, can be positively influenced by plasma nitriding. It was experimentally demonstrated that the diffusion

of nitrogen in the first stage of the gas nitriding process occurs mainly along the grain boundaries. This is understandable, considering that the catalytic disassociation of the ammonia gas on the surface of the steel would occur preferably, in areas of high energy. In intercrystalline diffusion, the nitrogen contacts the carbide phases in the grain boundaries. Due to the occlusion of nitrogen in the carbides, these begin to grow considerably and are, at the same time, converted into carbonitrides. This effect involves quite a waste of nitrogen and badly interferes with the grain boundary diffusion. For this reason the transcrystalline diffusion of nitrogen in gas nitriding (characterized by the formation of finely dispersed nitrides in the $\alpha$) is retarded.

On the other hand, most of the nitrogen is found to undergone transcrystalline diffusion right from the beginning of the process in plasma nitriding. This effect is due to the even condensation of the iron nitride from the plasma on the entire surface of the workpiece allowing a plane diffusion front to enter the whole material. Furthermore, the controllable partial sputtering of the carbon from the surface and the after-diffusion of carbon, mainly along the grain boundaries, cause something like decarburisation of the grain boundaries in the area close to the surface , so that those nitrogen atoms which diffuse along the grain boundaries cannot form any carbonitride phases which would inhibit further diffusion. An additional significant effect of the prevention of carbonitride precipitation in the grain boundaries close to the surface (up to 100 $\mu$m) lies in the considerable decrease in the brittleness of the nitride-hardened surface layers.

The two essential factors of the accelerated diffusion of nitrogen in plasma nitriding are the high surface concentration of nitrogen, which is of particular significance at the beginning of the process, and the increased rate of nitrogen penetration due to the different diffusion mechanism.

## 2.4 Structure And Properties of Plasma Nitrided Surface Layers

After plasma nitriding, the surface layers have essentially the same macroscopic structure as conventionally nitrided surfaces. There are, however, considerable differences with regard to microscopic details. The structure and possible layer modifications described below apply to plasma nitrided ferrous materials with a maximum of 10% of metallic alloying elements.

Fig.2.5 (a and b) shows the typical microstructure of plasma nitrided steel. The outermost layer, which is very thin and consists mainly of iron nitrides, is not attacked by an alcoholic nitric acid etch so that it is white on the micrograph. For this reason, the layer is usually referred to as "white layer". With regard to the structure and the special character of this layer, the more recent term "compound layer" is, however, more to the point. Beneath the compound layer is the so-called diffusion zone where the nitrogen has mainly been incorporated into the existing iron lattice as interstitial atoms or as a finely dispersed alloy nitride precipitate. The thickness of the diffusion zone depends on the temperature, time of treatment and the alloy content of the steel.

a)

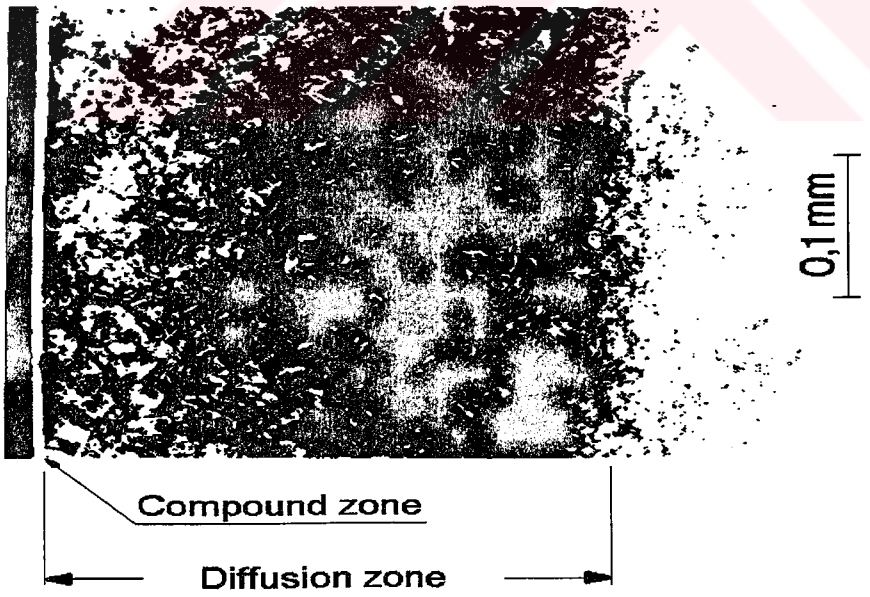

b)

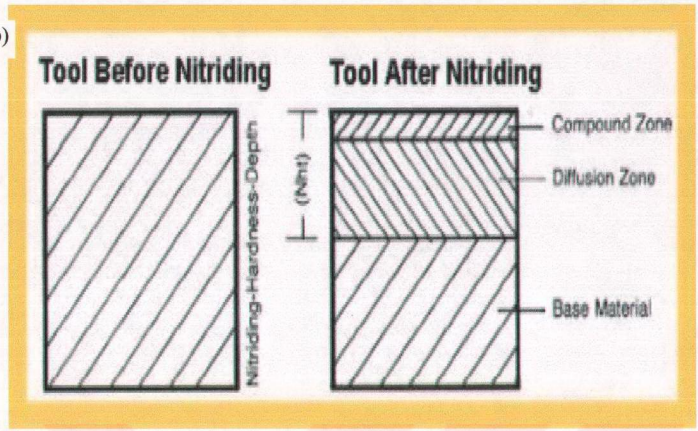


**Figure 2.5 Microstructural (a) and Schematic (b) presentation of the plasma nitrided tool.**

In contrast to conventional nitriding processes where, practically, only the thickness of these two zones can be varied within close limits, plasma nitriding offers the possibility of effecting several, precisely controllable, modifications to them, yielding very special properties. This ability to vary their structure is due to the great number of adjustable treatment parameters. The alteration of such parameters as voltage, current, gas pressure, gas composition, temperature, etc. has a direct influence on the fundamental physical phenomena of plasma nitriding. The different structure of plasma nitrided surface layers are usually achieved by means of the sputtering rate, which can be controlled by varying the voltage, or the pressure and composition of the gas mixture.

The properties of a plasma nitrided steel component are determined by both the core strength and the structural characteristics of the compound layer and the diffusion zone.

### 2.4.1 The Compound Layer

It is well recognized that for each fixed process condition there exist a critical nitrogen potential, called the threshold nitriding potential, below which an iron nitride layer does not form on the surface during plasma nitriding (Sun & Bell, 1991). In other words, reduction of the amount of available nitrogen at the surface during the process leads to complete suppression of compound layer formation (Lampe et al, 1993; Kovacs & Russell, 1986). Nitriding without iron nitride layer formation is usually called "bright nitriding".

By varying nitriding potential (i.e. $N_2$:$H_2$ ratio) for various times, threshold nitriding potential curves can be obtained experimentally for a given process temperature. The time required to obtain an iron nitride layer increases with decreasing nitriding potential. The time dependence of the threshold nitriding potential is in agreement with the fact that there exists an incubation time for the formation of the iron nitride layer. Indeed, during nitriding, the surface nitrogen concentration is built up gradually with time and the incubation time for the formation of the iron nitride layer is obviously the time necessary for the built up of the critical nitrogen concentration on the surface. Obviously, the threshold nitriding potential curve is temperature dependent. In the case of conventional gas nitriding it was observed that the curve moves upwards with increasing temperature, whilst in plasma nitriding the opposite trend was observed. This could be explained by the different nitriding and mass transfer mechanisms occurring in the gaseous and plasma processes (Sun & Bell, 1991).

When the nitriding potential ($N_2$:$H_2$ ratio) is above the threshold value, a compound layer consisting of $\gamma'$ ($Fe_4N$) and/or $\varepsilon$ ($Fe_{2-3}N$) will form on the surface of a steel component. It was experimentally demonstrated that even in carbon-free nitrogenous plasma a poly-phase ($\gamma'+\varepsilon$) compound layer was usually produced on the surface of low alloy steel. A monophase $\gamma'$ iron nitride layer can be produced only when the nitriding temperature is very high or the nitriding potential is sufficiently low. With decreasing nitriding temperature and time or increasing nitriding potential

the relative amount of ε phase formed in the compound layer is increased. The carbon content in the steel has a significant influence on the phase composition of the compound layer. The ε:γ′ ratio in the compound layer increases with increasing carbon content in the substrate (Sun & Bell, 1991; Karamış, 1992). Similarly, the introduction of carbon-containing gases into the nitriding atmosphere (plasma nitrocarburising) results in a compound layer composed of mainly ε phase. By careful control of the carbon content in the plasma, it is possible to produce a monophase ε iron nitride layer which has superior resistance to seizure and scuffing (Edenhofer, 1974b; Sun & Bell, 1991).

The development of the iron nitride layer is determined by nitriding temperature and time as well as nitriding potential. Decreasing the nitriding potential in the nitriding atmosphere, leads to a considerable reduction in the thickness of the iron nitride layer. Therefore, an iron nitride layer of high quality and desired thickness can be readily produced by monitoring the flow rate of $N_2$ and $H_2$ to the chamber. However, the development of the iron nitride layer only approximated to a parabolic dependence on time for the first few hours of nitriding, until a limiting thickness is reached, beyond which no further growth is observed (Sun & Bell, 1991; Karamış, 1992; Edenhofer, 1974b). It is believed that cathode sputtering plays an important role in determining the growth of the compound layer. By controlling the rate of sputtering, the thickness of the compound layer can be preset to the optimum, i.e. the minimum value that enables the workpiece to cope with the anticipated working conditions (Edenhofer, 1974b).

Investigations related to structure and mechanical properties of plasma nitrided steels have shown that the usefulness of the compound layer depends mainly on two factors: the homogeneity of the nitride structure and the thickness of the layer. With regard to the homogeneity of the nitride structure, the mechanical properties were found to be considerably better if the compound layer consisted of only one nitride phase, i.e. either γ′ or ε nitride. In poly-phased compound layers, containing a heterogeneous mixture of γ′ and ε phases, there are high inherent stresses in the

transitional region between the different lattice structures (γ′: face centered cubic and ε: hexagonal) which may give rise to micro-cracks if even a slight external stress is superimposed. The brittleness of the compound layer produced by gas nitriding (always poly-phased γ′ plus ε) and the less brittle compound layer of bath nitrided workpieces (exclusively ε nitride) confirm the influence of layer homogeneity.

As far as the thickness of the nitride structure is concerned, it is well known that the ductility of the layer decreases with increasing layer thickness.

Based on these two factors, the optimum properties will be produced when the compound layer is mono-phased (practical experience showed that small amount of mixed phases are of secondary importance) and of the minimum thickness necessary to meet specific property requirements such as wear and corrosion resistance. Careful control of the plasma nitriding process enables these two conditions to be met quite easily (Edenhofer, 1974b).

The carbon content in the steel also has a significant influence on the development of the compound layer. Under the same plasma process conditions the compound layer thickness increases with increasing carbon content in the substrate. Increasing the carbon content in steel increases the amount of ε phase in the compound layer, thus giving rise to the growth rate of the layer (Sun & Bell, 1991; Karamış, 1992).

Although the absence of porosity was shown by Edenhofer (Edenhofer, 1974b) as an advantage of the plasma nitriding, Lampe et.al. (Lampe et.al., 1993) pointed out that during plasma nitriding fine pores can form in the grain boundary zones of the compound layer. However, no pore channels with a direct link to the surface (as occur with salt bath nitriding) were observed. They also observed that the pores were formed in both types of nitrides and the quantity and size of individual pores increased with length of treatment and in particular at higher processing temperatures.

Extremely high levels of porosity, as can sometimes occur with salt bath nitriding and which are desirable under certain circumstances for specific applications, can not be achieved by plasma nitriding, since the nitrogen content of the compound layers is too low and the corrosive effect of the salt bath is not present (Lampe et.al., 1993).

### 2.4.2 The Diffusion Zone

As a result of the diffusion of nitrogen from the surface towards the core of the steel, several reactions occur simultaneously in the diffusion zone. These include precipitation of metal nitrides, saturation of α-Fe lattices with nitrogen, residual stress generation, carbon redistribution and grain boundary phase formation.

Good hardening of the surface of alloy steels is obtained by means of a very intensive, finely dispersed precipitate of alloy nitrides. If the iron lattice contains sufficient dissolved alloy elements capable of giving rise to these nitrides, such as Al, Cr, Mo, V, etc., their precipitation is, in the main, governed by the supply of nitrogen and the nitriding temperature. In plasma nitriding, the nitrogen content of the iron lattice near the surface is very high due to the FeN condensation on the surface and the high proportion of transcrystalline nitrogen diffusion. Furthermore, this nitrogen content can be influenced by varying the composition of the treatment gas (Edenhofer, 1974b).

Most of the nitrogen atoms in the diffusion zone (nitrided case) combine with chromium in the investigated Fe-Cr-C steels to precipitate CrN, which is the main cause of the hardening effect induced by nitriding. The generation of compressive residual stresses in the nitrided case is the result of saturation of nitrogen in α-Fe and precipitation of metal nitrides, i.e. CrN. The compressive stresses and the uptake of nitrogen in the nitrided case cause carbon redistribution: the carbon atoms initially in the steel will diffuse to the stress-free regions, i.e. towards the surface and the nitriding front, leading to the decarburisation of the nitrided case, the formation of a

carbon-rich zone in the nitriding front and the formation of a grain boundary phase parallel to the surface.

The hardness profile produced by nitriding reflects the quantity, size and distribution of fine scale of CrN precipitates, which are dependent upon the nitriding temperature and concentrations of chromium and carbon in the steel as well as the nitriding potential. Optimum hardness can be achieved at temperatures around 500°C. Reducing the nitriding potential ($N_2$:$H_2$ ratio) below the threshold value leads to a significant drop in the hardening effect owing to the relatively low nitrogen uptake in the diffusion zone. Increasing carbon content of the substrate decreases the hardening effect as well. the more carbon in the steel, the more chromium is tied up in the form of carbides: thus less chromium is immediately available to form CrN during nitriding and less hardness will develop.

The development of the nitrided case is a diffusion-controlled process. The case depth exhibit a linear relation with the square root of the nitriding time. However, when the nitriding temperature is near to or higher than the tempering temperature of the steel, the relation between the case depth and square root of the nitriding time may not be linear, particularly when the nitriding time is long.

The diffusion coefficient of nitrogen is reduced as the carbon content in the substrate is increased. Increasing temperature is more effective in enhancing the diffusion of nitrogen in low carbon steels than in high carbon steels. This is because more interstitial sites are occupied by carbon in high carbon steels.

During nitriding, the nitrided case tends to expand and is restrained by the unnitrided core. As a result, a compressive residual stress develops near the surface while a tensile residual stress evolves in the core (Jones & Martin, 1977). The level of residual stresses depends not only on the plasma process condition but also on the composition of the base material. Unalloyed carbon steels show comparatively small stresses after nitriding. However, plasma nitriding of the chromium-bearing steels

yielded much higher compressive residual stresses. The compressive residual stress in the nitrided case decreases with increasing carbon content in the steel, corresponding to the observed reduction of the hardening effect as the carbon content is increased. Nevertheless, no direct relationship between microhardness and residual stress level has been observed, although the origin of residual stress generation and hardness increase is similar i.e. nitrogen uptake and nitride precipitation (Sun & Bell, 1991).

Fig.2.6 shows the typical nitrogen and carbon concentration profiles of plasma-nitrided En40B steel. As a result of nitrogen uptake in the nitrided case, a decarburized zone near the surface and a carbon rich zone in the nitriding front have been developed. This phenomenon has been observed on both conventional and gas nitrided steel and plasma nitrided steel. However, decarburization of the nitrided case is more pronounced during the plasma process than during the gaseous process owing to the cathode sputtering involved in the plasma process. As a result, the precipitation of $Fe_3(N,C)$ phase in the prior austenite grain boundaries is less pronounced in plasma nitrided steel than in gas-nitrided steel. This may account for the high ductility of the plasma-nitrided case observed by Edenhofer (1974b). With increasing nitriding temperature and time and decreasing nitriding potential the extent of decarburization increases. This explains the observed variation of the ε:γ′ ratio in the compound layer with nitriding temperature, time and potential.

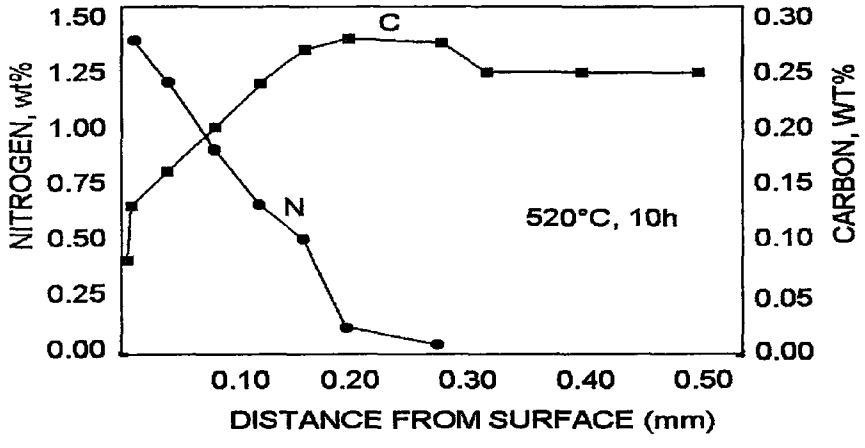


**Figure 2.6 Typical nitrogen and carbon concentration profiles of a plasma nitrided steel (Sun & Bell, 1991)**

## 2.5 The Advantages of Plasma Nitriding

The success of the plasma nitriding process led scientists in many countries to study the properties of plasma nitrided surface layers. All these studies independently agree on several major advantages of the process as compared to the conventional gas- or salt-bath nitriding techniques. The advantages most frequently mentioned can be summarized as follows:

- Completely environmentally harmless technology: Produce no toxic fumes or waste. There is no significant dirt, noise, or heat pollution
- No safety problems: There are no risks of explosion
- Reduced processing times (increased diffusion)
- Reduced energy consumption
- Reduced treatment gas consumption
- Reduced distortion
- No cleaning after the treatment.
- No grinding after the treatment
- Easy masking methods (selective treatment by using simple sheet masks)
- Treatment of the complete range of ferrous materials
- The ability to provide uniform case on complex geometry
- Superior, controllable, layer structures
- Increased service life
- The ability to impart hard wear resistance surfaces without brittleness or causing spalling or galling found with conventional nitriding
- The potential for reducing scrap through precisely repeatable cycles.

## 2.6 Industrial Applications of Plasma Nitriding

In spite of excellent laboratory results, a new process will only lend itself to industrial application if its control can be supervised or automated and if the results obtained at the laboratory stage can be reproduced on industrial plant.

Various industrial plasma nitriding installations have been available since 1970`s. As well as small automatic units for plasma nitriding small parts, e.g. 6million, the balls of ball-point pens with a diameter of about 0.7 mm per day, there are a number of large installations in which components weighing several tons can be treated. There is even examples of parts to be plasma nitrided as heavy as 14 tons in the literature (Edenhofer, 1976).

Today, large-scale industrial applications of plasma nitriding are mainly found in general mechanical engineering and in the fields of engine, vehicle, gear, roller and tool production(Figure 2.7). Some examples of applications are also given below :

**Figure 2.7 Nitriding applications of metal forming tools**

Side and middle housings of Wankel engines are plasma nitrided in series. For the purpose of plasma nitriding, the completely finished parts, which are made of GG 25 gray cast iron, are stacked on posts. The cooling ducts are covered with sheet-metal shields, so that only the rotor contact surface will be plasma nitrided. Dimensional changes due to plasma nitriding are extremely low. The change in dimension of the above-mentioned part is less than 20μm, measured across its entire contact surface. Thus, no refinishing is required. On the understanding that the workpieces have undergone a preliminary heat treatment (stress-relieving), this high dimensional stability is due to three specific properties of the plasma nitriding process:

1. Uniform, slow heating of the workpiece in the glow discharge.
2. Uniform temperature distribution during treatment due to a constant ion-current density over the entire surface of the workpiece.
3. Slow cooling in a vacuum.

The freedom from distortion that accompanies the plasma nitriding process is one such technical factor that has influenced design engineers in the automotive sector to specify plasma nitriding as an economic and technically viable alternative to the carbonitriding of timing gears which resulted in excessive scrap levels due to quench distortion problems.

Further examples typical of automotive components that are being routinely treated by the plasma nitriding method are illustrated in Fig.2.8. These comprise engine valves, differential housings for four wheel drive cars, differential rods for agricultural tractors, steering ball pivots, diesel injector bodies, and other engineering components. All these components are plasma nitrided under in line production conditions or in subcontract commercial heat treatment facilities (Rembges, 1986).

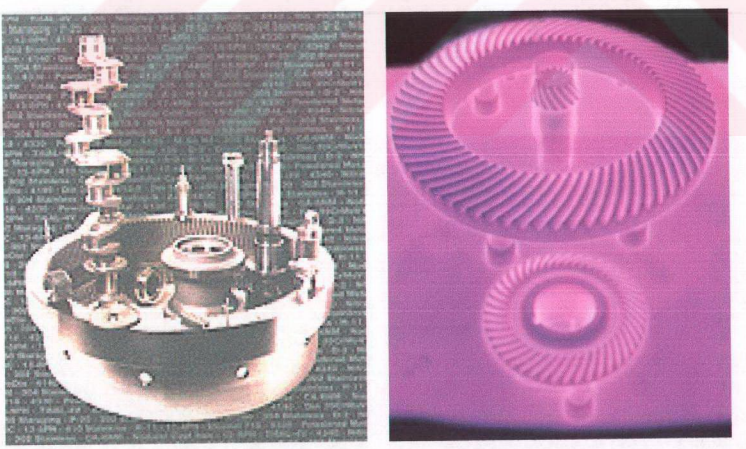

**Figure 2.8 Typical automobile or engine parts of which are routinely nitrided**

Plasma nitriding technique is also utilized in tool and die making. The process is applicable with advantage to all kinds of tools, whether they are intended for hot or cold working of metals, or for cutting, punching and chipping. The same holds true for the various tools used for the processing of plastics.

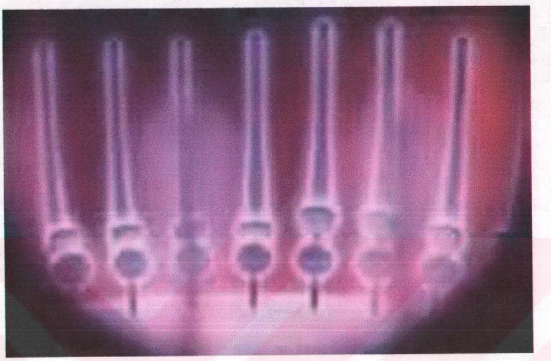

**Figure 2.9 Typical hip prostheses that are routinely plasma nitrided**

In the field of plastics processing machinery, the wear on extruding screws and cylinders has continued to increase because of the higher stresses exerted when processing thermoplastics and thermosetting plastics. Comparative measurements of the service life of gas nitrided and plasma nitrided equipment indicates that the plasma nitrided equipment lasts 5-12 times longer depending on the material. As well as small screws and cylinder, plasma nitriding furnaces have been produced capable of treating machine members up to 11m in length (Edenhofer, 1974b).

With forging dies, for example, which are usually made from hot working tool steels similar to H13, plasma nitriding treatments for 20 hours at 530°C, have been shown to give longer service lives than their 40 to 60 hour gas nitrided counterparts.

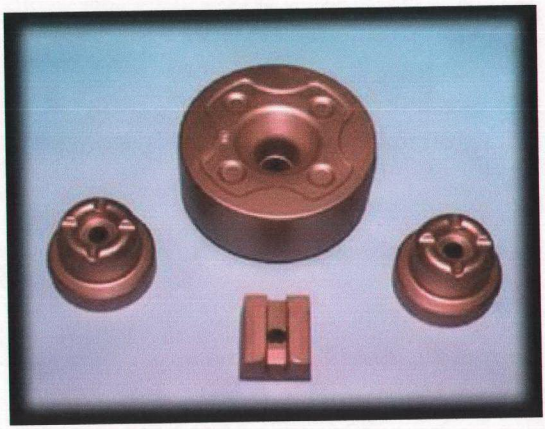

**Figure 2.10 Typical Plasma nitrided products**

With cold working tools for rolling, bending, drawing etc. it is vital that the high core hardness of the tools developed in hardening and annealing is not reduced by the subsequent nitriding treatment. For this reason, plasma nitriding treatment, which runs at temperatures as low as 400°C, offers new possibilities for nitriding of these components.

Such cutting tools as drills, taps, millers and punches are usually manufactured from high-speed steels and hardened and annealed to about 63 to 65 HRC. A plasma nitriding treatment of 10 to 30 minutes at 500°C will usually increase the surface hardness to about dph 1200. Naturally such an extremely hard layer has low ductility. Therefore, to keep embrittlement low, it is essential that only a thin diffusion layer without any compound layer is produced. This is achieved by choosing the appropriate treatment gas with a low nitrogen concentration, by keeping temperature low (500°C) and the treatment time short (10 to 30 minutes). This kind of treatment usually improves the service life of cutting tools by a factor of 2 to 4 (Edenhofer, 1976).

## 2.7 Economic Consideration

The economy and productivity of the process is another important point to mention. The advanced techniques used in controlling the vacuum, the dc currents and the glow discharge account for a capital cost of the plasma nitriding plant which is higher than that of a conventional gas- or salt-bath nitriding unit. However, when all other costs, i.e. running, maintenance, labor etc., as well as the through-put of the plasma nitriding installations is taken into consideration, a cost per part is arrived at which is competitive with conventional treatments.

The running cost of plasma nitriding installations are governed by the low consumption of gas and electric energy. Because treatment takes place in a vacuum, the necessary gas flow is as low as 30 to 100 l/h (7 to 20 g/h). The vacuum also accounts for the low energy consumption as the heat loss of the charge is by radiation only. The heat is directly produced at the surface of the workpieces by means of the ion bombardment and therefore the electric energy required to heat the charge depends on the size of its surface area. To plasma-nitride, for instance, a 14 ton En1g pressure bar pin to a depth of 0.02 in required an energy input of 3000 kWh. A load of very small pieces, for example 6000 inlet valves, weighing about 1 ton in total, takes an energy of about 400 kWh to be plasma-nitrided to a depth of 0.005 in (Edenhofer, 1976).

Maintenance costs are very small as there is no wear and no nitriding of the walls of the vessel. Corrosion is no problem either, as the gases used are not corrosive. In addition there are no heating elements subject to thermal shock and no moving parts except for a standard rotary vacuum pump.

The throughput of a plasma-nitriding installation is approximately three times that of a comparable gas nitriding unit, since overall treatment times are much shorter, while the quick and easy masking methods used in plasma-nitriding treatments are

other sources of appreciable cost and time savings. Additional considerable savings come after pieces leave the treatment vessel. Washing or cleaning is unnecessary.

To those cost savings, which are directly related to the working of plasma-nitriding installations, other indirect cost savings are to be added. They are produced by the longer service life, the special layer properties and the high dimensional stability. By this, machining and straightening processes are eliminated and secondary production costs as well as downtime are reduced.

All these factors add up to the positive economics of the plasma-nitriding process and have helped the fast growth of this technique within a sort time.

# CHAPTER THREE
# PROPERTIES OF STAINLESS STEEL

## 3.1 Types Of Stainless Steel

Stainless steel is a family of iron based alloys that must contain at least 10.5% Chromium (Cr). The presence of chromium creates an invisible surface film that resists oxidation and makes the material "passive" or corrosion resistant (i.e. "stainless"). This family can be simply and logically grouped into different branches. Each of these branches has specific properties and a basic grade or type. In addition, further alloy modifications can be made to "tailored" the chemical composition to meet the needs of different corrosion conditions, temperature ranges, strength requirements, or to improve weldability, machinability, work hardening and formability.

Stainless steel has been used as a standardized metal implant material since the 1920's when austenitic 18Cr-8Ni stainless steel alloys were succesfully used as implants. Fig.3.1

**Figure 3.1 Usage of stainless steel as an implant**

As a class of implants materials, stainless steels were chosen basically for their corrosion resistance and relative tissue compatibility. Currently, virtually all types of metal implants, including fracture plates, nails, screws, and joint replacement parts, are fabricated from austenitic stainless steel.

The most desirable composition of stainless steel would include a high concentration of Ni (12-17%) to comprimise adequate corrosion resistance and work hardening, a low concentration of C to prevent carbide formation, sufficient Cr for corrosion resistance, and a small concentration of Mo to resist pitting corrosion. The Mo content must be limited to prevent ferrite and sigma phase formation (embrittlement).The presence of Cr and Ni greatly modifies the Fe-C phase diagram. The stability of the austenite structure is one of the most important features of these stainless steels and is maximized by the solid solution of Ni and Cr in Fe. No hardening heat treatments are possible with austenitic stainless steels, since the martensite starting temperature is well below room temperature. In addition, the precipitation hardening does not occur in the standard commercial grade of these alloys. The addition of at least 8% Ni makes the austenite to martensite transformation very slow. These materials are therefore cold worked to supply added strength. Some martensitic changes, as evidenced by increasing magnetic character, can occur after extreme cold working.

Stainless steels are perhaps the easiest metal implant materials to fabricate; however, strickcare is required for the manufacturing of quality implant specimens. Altough it is possible to cast these materials to shape, the impurity levels produced by this technique lead to inferior corrosion and mechanical properties compared with forged and cold-worked products. Electric arc furnaces are used for melting, and subsequent vacuum arc melting techniques are often used to remove excess impurities such as C,Si,and Mn.

Austenitic stainless steels can be hot worked, but a noncarburizing, nonoxidizing atmosphere is required. The temperature range needed to accomplish this task is narrow. Most often, the heat treatment of choice involves quenching from 1050°C. This process will prevent formation of surface oxides and carbide precipitates (at 950°C). Carbides ($Cr_{23}C_6$) generally form at the grain boundaries due to interstitial

diffusion of C and are implicated in the rapid intergranular corrosion that can occur in stainless steels. Formation of σ phase due to Cr depletion in adjacent areas may be associated with carbide formation.

**Table 3.1 Mechanical Properties of different types of annealed stainless steels**

| MECHANICAL PROPERTIES (ANNEALED CONDITION) | | | | |
|---|---|---|---|---|
| STAINLESS STEEL | TENSILE STRENGTH MPa | YIELD STRENGTH MPa | ELONGATION in 2" | HARDNESS Rockwell B |
| 410 | 483 | 310 | 25 | 80 |
| 430 | 517 | 345 | 25 | 85 |
| 304 | 579 | 290 | 55 | 80 |
| 316 | 579 | 290 | 50 | 79 |
| 316L | 550 | 280 | 50 | -- |

Stainless steels are used for both corrosion and heat resisting applications. A three numeral numbering system is used to identify stainless steels. The last two numerals have no particular significance, but the first numeral indicates the group as follows:

**Table 3.2 Numbering system used to identify stainless steels ( Avner S.H., 1974)**

| SERIES DESIGNATION | GROUPS |
|---|---|
| 2XX | Chromium-nickel-manganese; non-hardenable, austenitic, nonmagnetic |
| 3XX | Chromium-nickel; non-hardenable, austenitic nonmagnetic |
| 4XX | Chromium; hardenable, martensitic, magnetic |
| 4XX | Chromium; non-hardenable, ferritic, magnetic |
| 5XX | Chromium; low chromium, heat resisting |

### 3.1.1 Cast Stainless Alloys

Cast stainless steels do not fall conveniently into any one of the stainless steel types because the vary somewhat from the chemical compositions of wrought alloys. The reason for this is that to be castable, an alloy must have a higher silicon content.(Wrought alloys are usually limited to 1% Si.) The additional silicon content is required particularly for thin cast sections. Also, high ferrite content is acceptable in cast products because rolling and forming is not required. Because the ferrite content in an austenite matrix substantially increases strength, such mixed structures of ferrite and austenite would cause great difficulty in rolling and forming if an attempt was made to treat these alloys as wrought alloys, therefore limiting this type of stainless steel to the cast form(Parr&Hansan, 1965).

The amount of the ferrite phase in cast alloys is incresed by adding or increasing the amounts of ferrite formers, such as chromium and molybdenum, and/or by decreasing the amounts of austenite formers and stabilizers such as nickel, nitrogen, and carbon. They have unusual properties such as increased yield strengths. Since these alloys can have two distinct microstructures, they are called duplex alloys. The corrosion resistances of cast and wrought stainless steels of similar composition are considered equivalent in most environments (Landrum 1989).

### 3.1.2 Wrought Stainless Steels

#### 3.1.2.1 Martensitic Stainless Steels

Martensitic stainless steels contain chromium that acts as a ferrite former. It is hardenable by heat treatment, the same as carbon steel, because it can form martensite, which is a hard constituent. The corrosion resistance tends to be better in the hardened condition than the annealed condition. The corrosion resistance is generally not as good as austenitic or ferritic stainless steels. The martensitic steels AISI 420, 431, 440A, 440B, and 440C are used when high hardness coupled with corrosion resistance is required. These are designated also like:

1. Metallurgical structure - Martensitic
2. Grade: 410 (most used), 420 (cutlery), 440C (for very high hardness)
3. Unified Numbering System UNS S41000, S42000, S44004

### 3.1.2.2 Ferritic Stainless Steels

The ferritic stainless steels can not be hardened by heat treatment because they do not undergo a phase transformation at higher temperatures. These steels are excellent for high temperature service; however they do not show consistent structural strength at elevated temperatures, so stresses must be kept low. AISI 442 and 446 are generally used in heat treating equipment. AISI 430 was the original material of construction used by the chemical industry for nitric acid service; however austenitic stainless steels have largely supplanted AISI 430 for this service because of their better fabricability and lower corrosion rates. Ferritic stainless steel alloys have a substantial advantage over austenitic stainless steels because they generally handle stress corrosion cracking better, particularly when chlorides are present. Ferritic stainless steels are designeted by three different systems;

1. Metallurgical structure - Ferritic
2. Grade: 409 (high temperature), 430(most used)
3. Unified Numbering System UNS: S40900, S43000

### 3.1.2.3 Austenitic Stainless Steels

Austenitic stainless steels are essentially chromium-nickel-iron alloys, generally of a composition varying from 16 to 26% chromium and 6 to 22% nickel, with a maximum of up to 0.25% carbon. Other alloying elements such as molybdenum, vanadium, and titanium are also added to develop or intensify certain specific properties. The most widely used grade of austenitic stainless steel is the type '18-8' and contain from 17 to 19% chromium, 8 to 10% nickel, and up to 0.20% carbon. When from 2 to 4% molybdenum is added to the basic compositions, types 316 and 317 are obtained,

which show an improved corrosion resistance against pitting and a higher temperature strength (Landrum, 1989). Austenitic type stainless steels have the following characteristics:

They are not magnetic, can not be hardened by "heat treatment" but can be hardened by cold working, have the best corrosion resistance, can be easily welded, have excellent cleanabilityand hygiene characteristics, have exceptional resistance to both high and low temperature. Austenitic stainless steels should be described by three different systems shown below respectively;

1. Metallurgical structure - Austenitic
2. Grade: 304 (most used), 310 (for high temperature), 316 (for better corrosion resistance), 317 (for best corrosion resistance)
3. Unified Numbering System UNS:S30400, S31000, S31600, S31700

Chemical compositions of austenitic type stainless steel are given in Table 3.2.

**Table 3.3 Chemical composition of austenitic type stainless steels.**

| Grades | C% | Cr% | Ni% | Mn% | Si% | P% | S | Others |
|---|---|---|---|---|---|---|---|---|
| 201 | 0.15 | 16-18 | 3.5-5.5 | 5.5-7.5 | 1 | 0.06 | 0.03 | 0.25 N |
| 301 | 0.15 | 16-18 | 6-8 | 2 | 1 | 0.045 | 0.03 | — |
| 302 | 0.15 | 17-19 | 8-10 | 2 | 1 | 0.045 | 0.03 | — |
| 303 | 0.15 | 17-19 | 8-10 | 2 | 1 | 0.2 | 0.15min | 0.6 Mo |
| 304 | 0.08 | 18-20 | 8-10 | 2 | 1 | 0.045 | 0.03 | 0.1 N |
| 308 | 0.08 | 19-21 | 10-12 | 2 | 1 | 0.045 | 0.03 | — |
| 310 | 0.25 | 24-26 | 19-22 | 2 | 1.5 | 0.045 | 0.03 | — |
| 316 | 0.08 | 16-18 | 10-14 | 2 | 1 | 0.045 | 0.03 | 2-3 Mo, 0,1N |
| 316L | 0.03 | 16-18 | 10-14 | 2 | 0.7 | 0.045 | 0.03 | 2-3 Mo, 0,1N |

Austenitic stainless steels hardness appreciably during cold working, but they can not be hardened by heat treatment. Recently austenitic stainless steels that can be hardened by the precipitation hardening have been developed. This is accomplished by adding such alloying elements as Cu, Ti, Be and Al, whose solubility in austenite decreases considerably as the temperature decreases, causing their precipitation on suitable heat treatment. Low nickel, high manganese austenitic stainless steels have been developed, designated as 201 type steel (Parr&Hanson, 1965).

Like the ferritic grades the austenitic stainless steels can not be hardened to form martensite by quenching. Whatever the cooling rate, they are austenitic at room temperature. Nor do they undergo a transformation on heating temperatures below the melting range.Thus, like the ferritic stainless steels, their grain size can not be controlled. However, grain growth is not so a great problem. While the ferritic stainless steels can be strengthened to some extent by cold working, this effect is not great and its extent is limited by the rather low ductility of the grade. However, the austenitic grades are much more ductile: they can suffer more cold work without breaking, and, further, during cold work, many members of the group undergo a transformation that is, in fact, martensitic. Thus we should expect to find substantial strengthening in many austenitic steels during cold working (Parr&Hansan, 1965).

Chromium is the resistant keystone of all the types of stainless steel. When the amount of chromium is gradually increased under oxidizing conditions, a surface film attempt to form and then it rather suddenly completes itself when about 12% chromium is present. The oxide layer at that concentration of chromium is tenacious and impenetrable to migrating atoms, either oxygen atoms pressing inward or metallic atoms pressing outward, thus passivating the corrosion action. When this strong, continuous film has been formed, the metal is in the passive state (Landrum, 1989).

As nickel is prograsively added to a ferritic stainless steel containing 18% chromium, the stability of austenitic phase increase until the steel becomes austenitic at all temperatures. For a steel with 0.1% carbon a completely austenitic structure is obtained with 7% nickel. The structure, however, becomes complicated because of the

presence of chromium carbides. They have very small solubility below a temperature of 982°C and precipitate preferentially along the grain boundaries. The microstructure of a steel with less than 7% nickel will consist of austenite, ferrite, and chromium carbides, whereas that of a steel with minimum 7% nickel and more will consist of austenite and precipitated carbides.

Another method of obtaining a stable material would be to eliminate completely the carbon from the steel. This is impractical and too expensive, but lowering the carbon content below 0.03% is possible and will decrease the danger of chromium carbide precipitation. Extra low carbon austenitic stainless steels (such as 316L) containing a maximum of 0.03% carbon have been developed, which give satisfactory performance without full annealing of the lubricated and welded pieces (Parr&Hanson, 1965).

Another structural phase observed in austenitic stainless steels and in some ferritic stainless steels is the 'sigma' phase (σ). The sigma phase is a hard and brittle intermetallic compound of variable compositions that affects adversely the ductility and corrosion resistance of the stainless steel. It is believed that this sigma phase is formed from ferrite, preferably at the edges of ferrite grains. Steels with a Cr content above 20%, containing such ferrite-forming elements as Mo, Co, Ti, and W, are susceptible to the sigma-phase formation. On the other hand an increase in the Ni content retards the sigma-phase formation. Consequently, the Ni content of type 316 stainless steel, containing from 2.5 to 3% Mo, must be raised 10% in order to prevent the formation of the sigma-phase (Parr&Hanson, 1965).

### 3.2.2.3 Precipitation-Hardening Stainless Steels

As a result of research during World War II a new group of stainless steels with precipitation-hardening characteristics were developed. The first of these nonstandard grades of stainless steels, 17-7PH, was made available in 1948. These steels are usually solution annealed at the mill and supplied in that condition. After forming they are aged to attain the increase in hardness and strength. In general they have lower nickel content, thus reducing the stability of the austenite. These steels may also have

elements such as copper and aluminum that tend to form coherent alloy precipitates (Avner S.H., 1974).

### 3.3 Production of Stainless Steels

Stainless steel is produced in an electric arc furnace where carbon electrodes contact recycled stainless scrap and various alloy of chromium (and nickel, molybdenum etc. depending on the stainless type). Acurrent is passed through the electrode and the temperature increases to a point where the scrap and alloys melt. The molten material from the electric furnace is then transferred into an AOD (Argon Oxygen Decarbonization) vessel, where the carbon levels are reduced (remember stainless has a much lower carbon level than mild steel) and the final alloy additions are made to make the exact chemistry. Figure 3.2 shows the process from melting and casting either into ingots or continually cast into a slab or billet form. Then the material is hot rolled or forged into its final form. Some material receives cold rolling to further reduce the thickness as in sheets or drawn into smaller diameters as in rods and wire.

Most stainless steels receive a final annealing (a heat treatment that softens the structure) and pickling (an acid wash) that removes furnace scale from annealing and helps promote the passive surface film that naturally occurs).

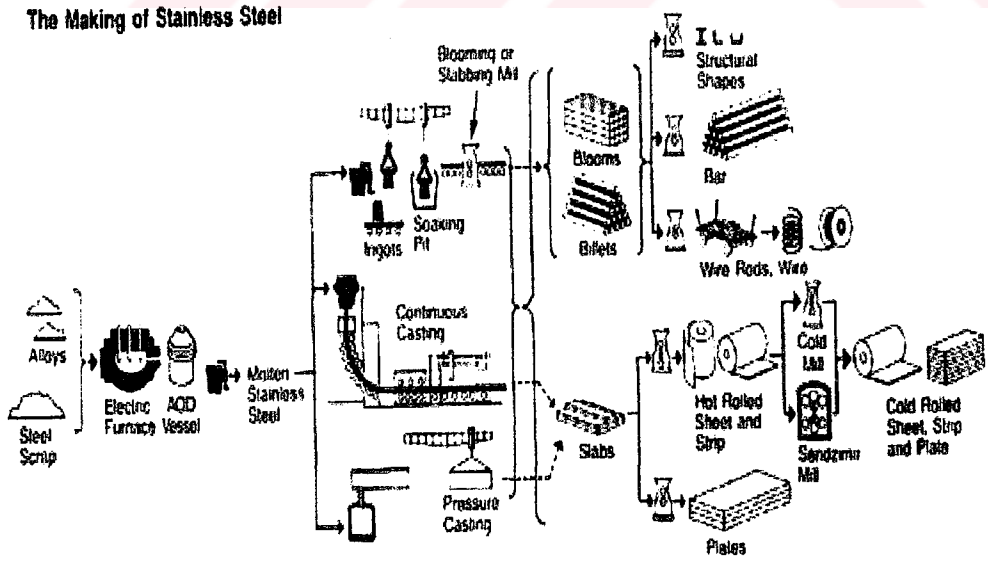


**Figure 3.2 Schematic representation of a stainless steel production**

### 3.4 Life Cycle

The fact that stainless steel has a great resistance to corrosion means that using stainless will result in a very long life compared to mild steel. Structures made from stainless will last many times the normal life (well over 100 years in most cases). So, while stainless steel is probably more expensive to buy in the beginning and because it lasts a long time, it is usually cheaper in the long run because there is little or no maintenance and repair costs. And, once the useful life is over, stainless steel is 100% recyclable. Scrap stainless steel is recarged into the electric furnaces for re-melting back into stainless steel. So it can be seen that stainless steel is a true "full life cycle" material.

### 3.5 Benefits of Stainless Steel

Lower alloyed grades resist corrosion in atmospheric and pure water environments, while high alloyed grades can resist corrosion in most acids, alkaline solutions, and chlorine bearing environments, properties which are utilized in process plants.

Special high chromium and nickel alloyed grades resist scalling and retain strength at high temperatures.

The easy cleaning ability of stainless makes it the first choice for strict hygiene conditions, such as hospitals,kitchens,laboratories and other food processing plants. Also, the bright, easily maintained surface of stainless steel provides a modern and attractive appearance.

The work hardening property of austenitic grades, that results in a significant strengthening of the material from cold working alone, and the high strength duplex grades, allow reduced material thickness over conventional grades, therefore cost savings.Modern steel making techniques mean that stainless can be cut, welded, formed, machined, ans fabricated as readily as traditional steels. And finally, when the total life cycle costs are considered, stainless is often the least expensive material option.

# CHAPTER FOUR
# EXPERIMENTAL STUDIES

## 4.1 Material

Commercial AISI 316 L stainless steel was used as the test material and its chemical composition is listed in Table 4.1. As-received AISI 316L stainless steel rods, which had a diameter of 10 mm, the specimens were cut from in 10 mm length by using universal lathe. Our specimen's solid model shown in Figure 4.1

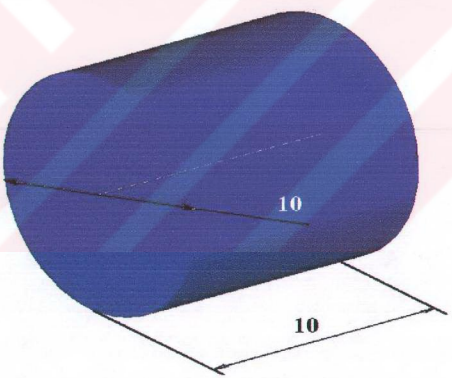


**Figure 4.1 AISI 316L stainless steel test specimens**

For the most part, the 316L stainless steels used for medical implants have adequate but not superior mechanical properties. Typical mechanical properties of these alloys are shown in Table 4.1

**Table 4.1 Mechanical Properties of AISI 316L Stainless Steel**

| PROPERTY | WROUGHT | CAST | COLD WORKED | ANNEALED |
|---|---|---|---|---|
| Elastic Modulus(MPa) | $1.9\text{-}2.1 \times 10^5$ | $1.93 \times 10^5$ | $2.0 \times 10^5$ | $2.0 \times 10^5$ |
| Shear Modulus(MPa) | $8.4 \times 10^4$ | -- | -- | -- |
| Yield Strength(0.2%) | $2.05\text{-}2.4 \times 10^2$ | $2.06 \times 10^2$ | $7.5\text{-}7.9 \times 10^2$ | $2.8 \times 10^2$ |
| Ult. Tensile Strength(MPa) | $5.1\text{-}5.5 \times 10^2$ | $4.82 \times 10^2$ | $9.6\text{-}10 \times 10^2$ | $5.5 \times 10^2$ |
| %Elongation | 55 | 30 | 9-22 | 50 |
| Poisson's ratio | 0.283 | -- | -- | -- |
| Fatique Endurance L.(MPa) | -- | -- | $3.0 \times 10^2$ | $2.3\text{-}2.8 \times 10^2$ |
| Hardness(Rockwell B) | 70-95 | | | |

Fully annealed (softened) stainless steels exhibit a fairly high ultimate tensile stress; however, the proof (yield) stress is low and the ductility is high. As a result, plastic deformation occurs quite readily with these materials.

These alloys can be strengthened by cold working. The effects of cold working on the mechanical properties can be seen from the Table 4.1. Cold working does not change the elastic modulus, but does increase yield and ultimate strengths.Mechanical properties of our cold worked test materials (AISI 316L) such as yield stress ($\sigma_y$), ultimate tensile strength ($\sigma_{uts}$) and elongation ($\varepsilon$) were determined as 750 MPa, 960 MPa, and 20% respectively.

**Table 4.2 Chemical composition of test material (AISI 316 L)**

| ELEMENTS | Si | Mn | Cr | Ni | Mo |
|---|---|---|---|---|---|
| | V | Cu | P | S | Nb |
| | Ti | Co | C | Al | Fe |
| TYPE 316L %wt | 0,1756 | 1,6301 | 17,5512 | 13,9588 | 2,9370 |
| | 0,0163 | 0,0455 | 0,00 | 0,0145 | 0,00 |
| | 0,0031 | 0,0512 | 0,0152 | 0,08 | 63,522 |

After heat treatment, for metallographic examination & microhardness testing and wear testing, specimens were machined and ground.

### 4.2 Plasma Nitriding Procedures

The plasma nitriding was carried out in a laboratory type plasma-nitriding unit (Fig.4.2) produced in Mechanical Engineering Department of Dokuz Eylül University. The unit did not allow the direct control of the current of the glow discharge. In all the treatments the surface area of nitrided components were kept constant, so current density is proportional to current. The voltage and current density ranges were 400-600V and 2.5-4.0 $mA/cm^2$ depending upon the gas composition of the plasma atmosphere and required temperature. Plasma current was increased by increasing the applied voltage and increasing the $N_2$ concentration of the nitriding atmosphere. Upper values of applied voltage were utilized in the case of lower nitrogen concentrations and higher treatment temperatures.

a)

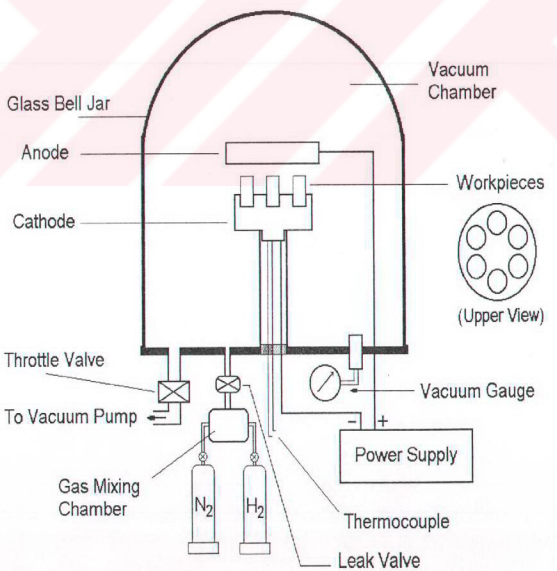

b)

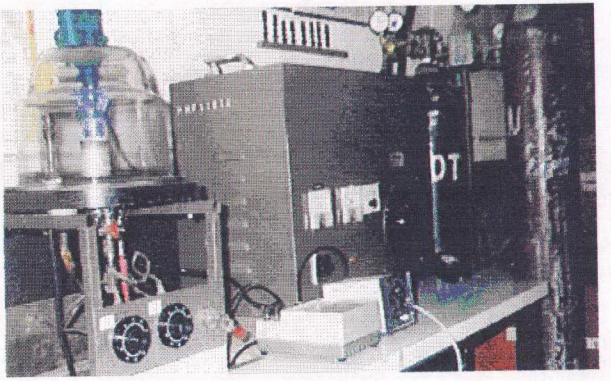

**Figure 4.2 Dokuz Eylül University Plasma-nitriding research and application unit. a) Schematic b) Photographic**

The plasma nitriding process was performed as follows:

1. After cleaning in alcohol, the specimens were put into the plasma nitriding chamber and the chamber was evacuated to $2x10^{-2}$ mbar.
2. Prior to plasma nitriding, the samples were subjected to cleaning by hydrogen sputtering for 15 minutes under a voltage of 600 V and a pressure of 5 mbar to remove surface contaminants.
3. Gas mixture containing predetermined volume of Nitrogen and Hydrogen was allowed to flow into the chamber.
4. The pressure inside the chamber measured with the manometer was maintained at 10 mbar by balancing the leak rate against the vacuum pump.
5. The power supply was switched on and the voltage gradually incrased to strike a glow. Then, it was further increased to heat the specimens to the required temperature.
6. The temperature was monitored by a Ni-CrNi thermocouple inserted through the hole at the bottom of a specimen. Due to the symmetry of the specimens about the cathode axis, this temperature reading was accepted to be the temperature of all specimens being plasma nitrided together.

7. Time keeping for the process was started as soon as reaching the process temperature which took about 15 minutes after the formation of plasma.
8. All of the plasma nitriding procedures were carried out at various temperatures, times and gas compositions. Table 4.3 shows their variations relative to each other. A total gas pressure of 10 mbar was kept constant throughout the study.
9. The specimens were cooled to room temperature slowly in the vacuum atmosphere, before they were removed from the vacuum chamber.

**Table 4.3 Plasma nitriding process conditions.**

| GROUP | TİME (h) | TEMPERATURE (°C) | NITROGEN (vol. %) |
|---|---|---|---|
| 1.400.40 | 1 | 400 | 40 |
| 1.500.40 | 1 | 500 | 40 |
| 4.400.40 | 4 | 400 | 40 |
| 7.400.40 | 7 | 400 | 40 |
| 10.400.40 | 10 | 400 | 40 |
| 4.500.40 | 4 | 500 | 40 |
| 4.500.50 | 4 | 500 | 50 |
| 7.500.40 | 7 | 500 | 40 |
| 10.500.50 | 10 | 500 | 50 |
| 4.550.40 | 4 | 550 | 40 |
| 7.550.40 | 7 | 550 | 40 |
| 10.550.50 | 10 | 550 | 50 |
| 4.600.40 | 4 | 600 | 40 |
| 7.600.50 | 7 | 600 | 50 |
| 10.600.40 | 10 | 600 | 40 |

### 4.3 Microhardness Testing and Optical Microscopy

After the completion of plasma nitriding process, the cross-sections, were mounted in a bakelite, prepared using standard techniques of Struers bakelite machine.The surfaces of all samples were ground by SiC emery paper in a sequential order starting from 600 down to 1200. After grindind, each specimen was polished with a diamond

paste of 1μm until all micro scratches were eliminated. In the next stage, the chemicals and the left-overs on the specimen surface were washed away with a warm soapy water and the specimens were dried by blowing dry air.

The most and the last important stage in the microscopic structural examination is etching with an acidic solution. The two significant parameters in etching are the time of etching and etchant itself. Etching is a chemical process of selective dissolution of the surface with a suitable reactive reagent. The composition of the etching solution used to etch 316L stainless steel is follows: 28% $HNO_3$, 42% HCl, 28% $CH_3COOH$, 2% Glycerine. The specimens were exposed to the etching solution (40 minutes after its preparation) and left exposed to it for an average of 3 to 4 seconds enough to reveal a discernible microstructure. Subsequently specimens were taken out of the solution, washed in hot water and cleaned with soap and finally, dried in hot air in order not to leave any reactant. Afterwards the prepared samples were kept stored in a desiccator until they were used.

The structures were observed and photographed using an optical microscope. The thickness of compound layers were also measured during these observations.

Vickers microhardness measurements using a load of 80 gr were performed to determine case depth as well as to aid in characterizing the physical properties of the case as a function of depth from surface. Case depth at a hardness value 10% above the core hardness was taken as an accurate measure of total case depth. Vickers hardness values are calculated with using the formula written in below.

$$\text{Vickers Hardness (HV)} = \frac{1855 \times 80}{(0.292 \times X)^2}$$

Average hardness values of a minimum of three indentations at each depth were used to obtain microhardness profiles of the specimens.

Optical microscopy was also employed in fractography studies of worn surfaces.

## 4.4. Wear Testing

Wear is one of the most commonly encountered industrial problems leading to the replacement of components and assemblies in engineering. Though rarely catastrophic, it reduces the operating efficiency by increasing power loses and the rate of component replacement. Hence evaluation of the wear characteristics of engineering materials is very essential in order to have a better understanding of the factors which most influence it and also enable maximum utilization of the materials.

The wear specimens were tested under dry (unlubricated) conditions in accordance with ASTM G99 standards using pin-on-disc sliding wear testing machine, as can be seen below, which is founded in Dokuz Eylül University Mechanical Engineering Department.

Wear tests were performed on untreated and plasma nitrided specimens to determine the optimum process parameters or microstructure for maximum resistance to wear. All wear tests were caried out under dry sliding conditions at room temperature using a pin-on-ring types of wear testing machine shown in Fig.3.4. The ring of wear couple was made of an oil quenched AISI 4140 steel having a hardness of 65±2 HRC. It had a diameter of 140mm, and a thickness of 16mm. The cylindrical surfaces of the rings were ground to a surface finish of 0.20μm (Ra).

A standart test procedure was employed. Pins of the material under investigation were cylindrical samples 10 mm in length and 10 mm in diameter. After machining, flat faces of the pins were ground using 600 grit SiC emery paper.

Tests were performed with a normal load of 40 N ($P_N$), and a sliding speed of 0,5 $m.s^{-1}$ (200 rpm) for a total sliding distance of 15000 m. The tests were interrupted after each 500m of sliding distance so that the wear rate of the pins could be monitored by weight loss to an accuracy of $\pm 10^{-4}$g. Pins and rings were cleaned with alcohol before the tests. The pins were also cleaned in the same way before and after each weighing.

The wear results were computed from weight loss measurements. The data for the wear tests was taken from the average of two measurements. The standard deviation was about 5%. Since the hardness of the counterface (steel disc) was fairly equal with the specimens, the wear properties of the steel disc are not studied in the present work.

After the wear tests, wear scars were examined by optical microscopy to monitor topographic features of worn areas and to investigate whether any change in wear behaviour occured as a result of plasma nitriding. Wear debris was collected and examined by optical microscopy as well.

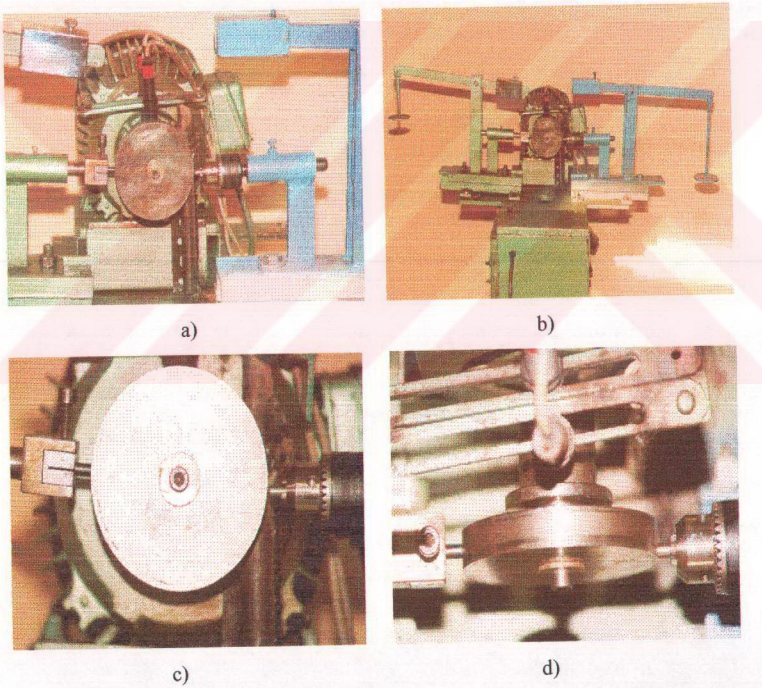


**Figure 4.3 The four external appearances of Dokuz Eylül University wear testing machine**

# CHAPTER FIVE
# RESULTS AND DISCUSSION

## 5.1 Microstructure and Microhardness

Microstructural examination of plasma nitrided specimens showed formation of compound layers with different thicknesses indicating that nitriding potentials (i.e. $N_2$:$H_2$ ratio) of all groups were above the threshold value below which an iron nitride layer does not form on the surface. Effect of process temperature, duration, and nitrogen content of the plasma nitriding atmosphere on compound layer thickness can be observed on micrographs given in Figure 5.1.

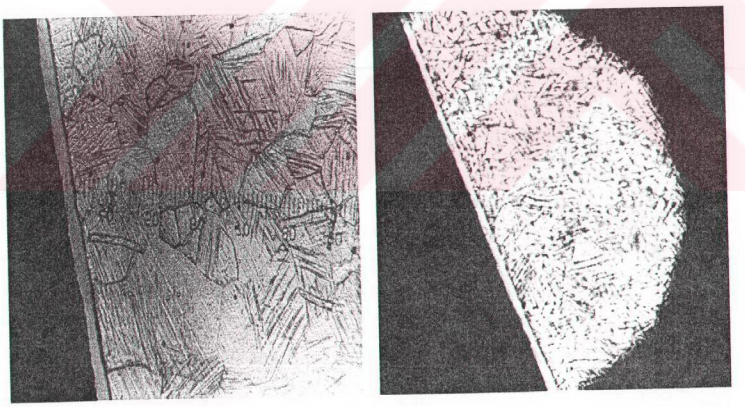

a b

**Figure 5.1 Cross-sectional optical micrographs of plasma nitrided samples a) 7.400.40 at x450 magnification b) 7.400.40 at x200 magnification (etch : %28 $HNO_3$ + %42 HCl + %28 $CH_3COOH$ + %2 Glycerine)**

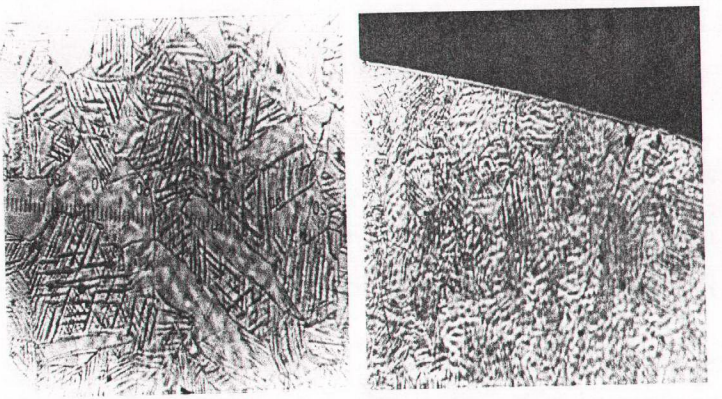

a b

**Figure 5.2 Cross-sectional optical micrographs of plasma nitrided samples a) 1.400.40 at x450 magnification b) 1.400.40 at x200 magnification**

It is found that compound layer exists for 400°C treatments. Compound layer thickness for 1h, 4h and 7h treatments ( at 400°C and vol. 40%$N_2$ ) are 3.07 μm, 9.21μm and 23.52 μm respectively.

It is clearly seen that compound layer thickness increases by increasing all these three parameters just for 400°C process conditions. Process temperature seems to be the most effective parameter in determining the compound layer thickness. So compound layer does not exist at 500, 550 and 600°C conditions or its very little to measure with our technical equipment. Beside the process temperature volumetric ratio of $N_2$ is the other effective parameter in determining the compound layer thickness. From our experiments we found that 40% $N_2$ volumetric ratio is the saturation value for compound layer formation.

The compound layer which has a thickness of approximately 9.21μm is clearly visible on the Figure 5.3. This photograph represents the treatments that we have done at 4 h 400°C and 40%$N_2$ process conditions. Transition from compound layer to the main material is also seen from this photograph.

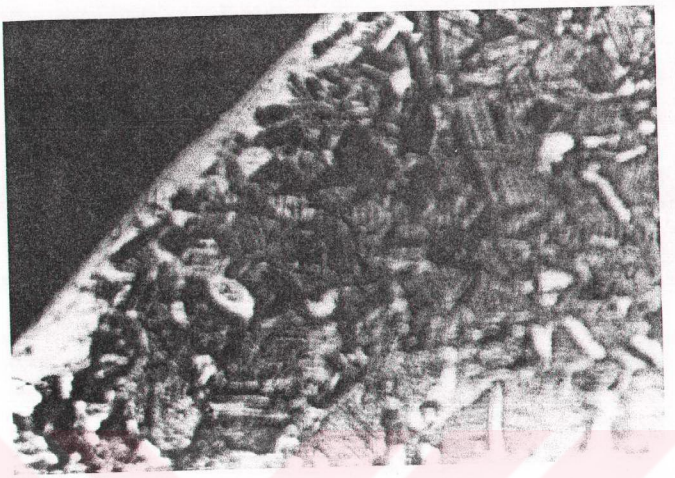

**Figure 5.3 Compound layer thickness and the transition to the main element shown above for the 4.400.40 process condition at x200 magnification**

Average microhardness values as well as case depths, compound layer thicknesses and case hardness are represented in Table 5.1, Figure 5.4 and Figure 5.5 for the 15 groups of specimens considered in the study.

Case depths have been determined from the hardness-depth values by interpolation using the definition given in Section 2.3. Case depth profiles as a function of process conditions are shown in Figure 5.4.

It is clearly seen from the Figure 5.4, the case depth increase with increasing temperature. In fact there is an exceptions on the 600°C conditions. As its seen when the gaseous consumption is changed from %40 to %50 vol.$N_2$ the case depth is slightly decreased even time increase (Figure 5.15).

Figure 5.5 is shown the case hardness profiles of specimens. The maximum hardness is gained at 7.550.40 process conditions. We have found that case hardness is suddenly decreased when the temperature is increased to the 600°C.

**Table 5.1 Average values of microhardness corresponds to the distance from the surface of all specimen groups**

| | MICROHARDNESS (HV) | | | | | | | | | |
|---|---|---|---|---|---|---|---|---|---|---|
| | DISTANCE FROM SURFACE (μm) | | | | | | | | | |
| **GROUP** | **30** | **80** | **150** | **250** | **350** | **500** | **700** | **1000** | **1200** | **1500** |
| **1.400.40*** | 355 | 355 | 355 | 355 | 355 | 355 | 335 | 335 | 335 | 335 |
| **1.500.40** | 1087 | 1087 | 1087 | 1035 | 1035 | 1035 | 619 | 365 | 335 | 335 |
| **4.400.40** | 1087 | 1087 | 1035 | 1035 | 1061 | 724 | 387 | 355 | 335 | 335 |
| **7.400.40** | 376 | 376 | 345 | 345 | 345 | 345 | 335 | 326 | 335 | 335 |
| **10.400.40** | 411 | 411 | 355 | 355 | 355 | 355 | 355 | 345 | 345 | 345 |
| **4.500.40** | 1342 | 1342 | 1342 | 1342 | 1342 | 1342 | 1010 | 355 | 345 | 335 |
| **4.500.50** | 1342 | 1342 | 1342 | 1342 | 1342 | 1342 | 1010 | 450 | 345 | 335 |
| **7.500.40** | 1462 | 1462 | 1462 | 1462 | 1462 | 1462 | 1035 | 452 | 355 | 335 |
| **10.500.50** | 1342 | 1342 | 1342 | 1342 | 1205 | 822 | 345 | 335 | 335 | 335 |
| **4.550.40** | 1505 | 1420 | 1420 | 1420 | 1342 | 1342 | 1205 | 381 | 340 | 335 |
| **7.550.40** | 1699 | 1699 | 1699 | 1699 | 1699 | 1699 | 1699 | 1699 | 1342 | 335 |
| **10.550.50** | 1462 | 1420 | 1420 | 1462 | 1462 | 1205 | 1174 | 335 | 335 | 335 |
| **4.600.40** | 1342 | 1342 | 1342 | 1342 | 1342 | 1342 | 1205 | 382 | 345 | 335 |
| **7.600.50** | 1271 | 1271 | 1205 | 1205 | 1035 | 1035 | 585 | 335 | 335 | 335 |
| **10.600.40** | 1061 | 1035 | 1035 | 1035 | 1010 | 1035 | 1035 | 1010 | 755 | 355 |
| **Untreated** | 335 | 335 | 335 | 335 | 335 | 335 | 335 | 335 | 335 | 335 |

(* see table 4.3 for the process conditions of the groups)

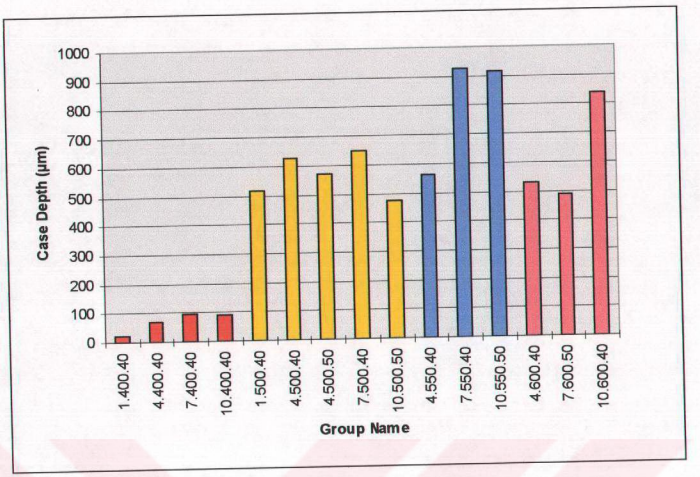


**Figure 5.4 Average case depth of our specimen groups**

The microhardness profiles as a function of depth from the surface are shown in Fig.5. 5 for all of the specimen groups.

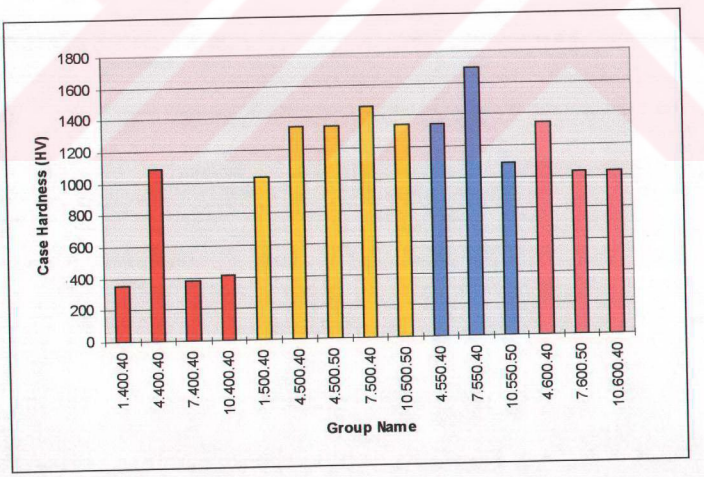


**Figure 5.5 Case hardness profiles of specimens**

Significant surface hardening have been observed in all plasma nitrided samples. The maximum hardness levels, the shape of the hardness-depth profiles obtained in the study are understandable.

Effects of process parameters such as treatment temperature, duration, and nitrogen content of the atmosphere (vol.%$N_2$) on the hardening characteristics of the specimens have been discussed below.

In addition to hardness-depth curves, graphics illustrating the variations of surface hardness, case depth, and compound layer thickness versus process parameters have been presented. The surface hardness values are the ones measured at nearly 30μm below the surfaces of cross sectional specimens, i.e. the first values of the hardness-depth curves.

The effect of treatment time on the hardness behavior of the plasma nitrided samples treated at 400°C is shown in Figure 5.6. There does not seem any valuable hardness increase for 400°C treatments. Because of this 400°C is not a good parameter for plasma nitriding surface hardening process.

The effect of treatment time on the hardness behavior of the plasma nitrided samples treated at 500°C is shown in Figure 5.7. Hardness level, case depth, and compound layer thickness are strongly affected by the process time. The maximum hardness level is observed for a treatment time of 4h 550°C and a decrease in hardness occurred for longer duration (shown in Figure5.9).

The effect of gas compositions on the hardness behavior of the plasma nitrided samples treated at 500°C is shown in Figure 5.15. Hardness level is affected by the gas composition. Here %40$N_2$+%60$H_2$ composition gives better microhardness values and larger diffusion layer thickness against %50$N_2$+%60$H_2$ gas composition at 4 hour 500°C process conditions.

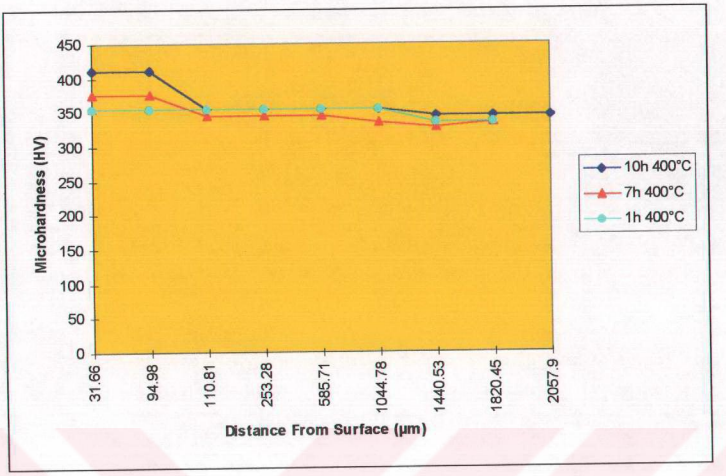


**Figure 5.6. The effect of treatment time on the hardness behavior of the plasma nitrided samples treated at 400°C**

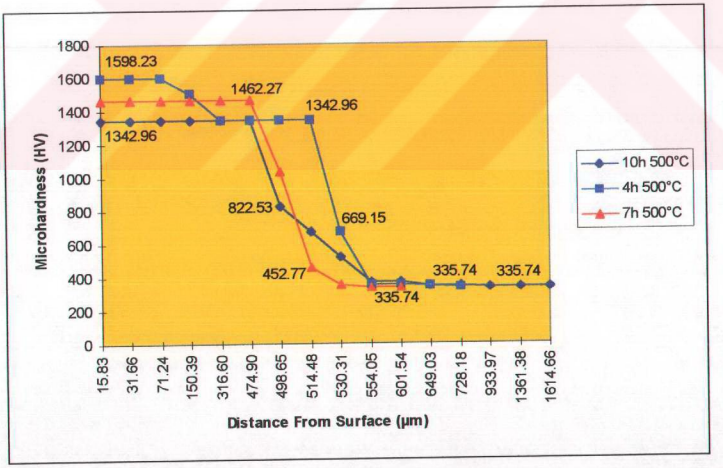


**Figure 5.7. The effect of treatment time on the hardness behavior of the plasma nitrided samples treated at 500°C**

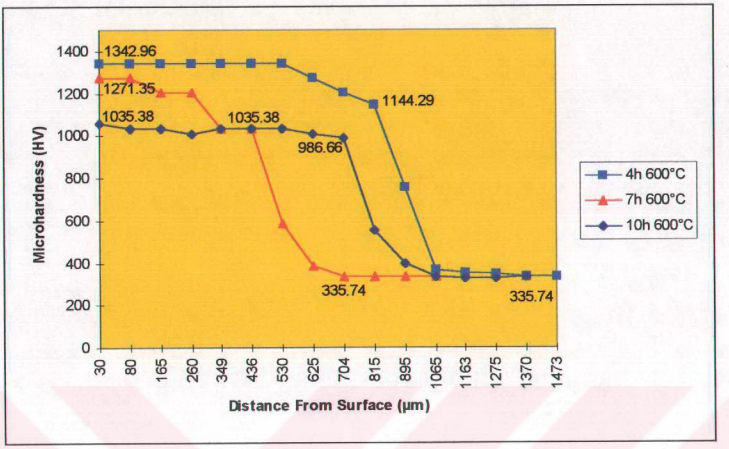


**Figure 5.8. Microhardness-depth profiles of samples plasma nitrided for 4,7,10 hour at 600°C**

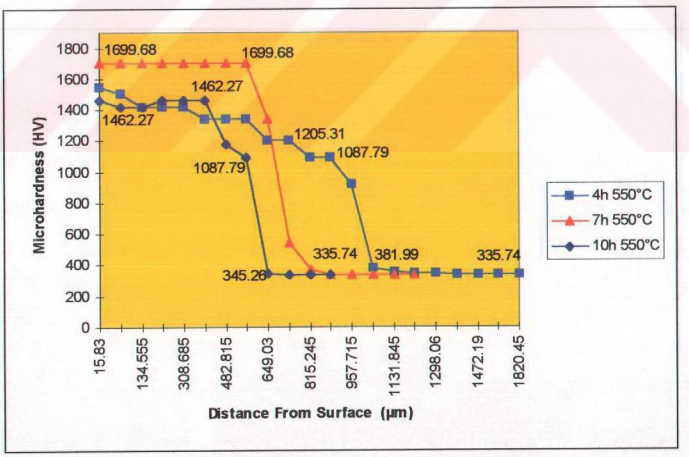


**Figure 5.9. The effect of treatment times on the hardness behavior of the plasma nitrided samples treated at 550°C**

The time dependence of surface hardness is thought to be a result of precipitate size and density. For the shortest time (1h) the nitrogen uptake and precipitate density are low and therefore the amount of hardening is also low. For longer treatment times both precipitate growth and tempering of the matrix become important. As has been observed in many precipitation hardening alloys, a maximum in hardness is achieved, which corresponds to a particular aging time and temperature. This hardness is in turn related to both precipitate density and precipitate size (Robino & İnal, 1982).

Therefore, with regard to the process time, the sample plasma nitrided over a period of 7h (at 550°C) produces an optimum nitride precipitate size and density. Surface hardness of samples treated for longer duration decreased due to the coarser precipitates.

The surface hardness are found to be parabolic with time (Figure 5.10). Compound layer thickness does show an increasing trend with increasing time, but it seems to reach a saturation. The saturation may be explained by surface sputtering which causes decarburisation of the surface leading to transformation of iron-nitrides from ε to γ′. This transformation has a limiting effect on compound layer thickness. Also the saturation is related with the volumetric ratio of $N_2$ gaseous in the vacuum furnace.

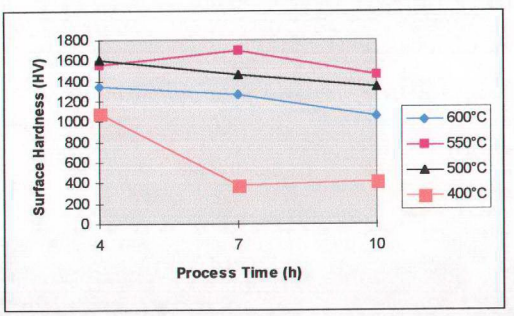


**Figure 5.10. Surface hardness changes as a function of plasma nitriding times (for both 400°C, 500°C, 550°C and 600°C experiments).**

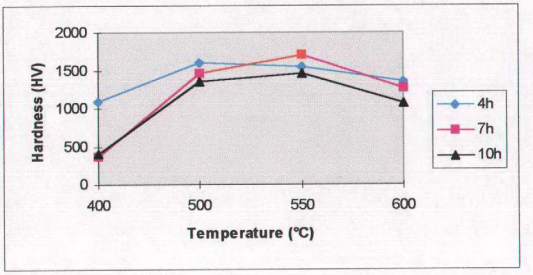


**Figure 5.11. Surface hardness changes as a function of plasma nitriding temperatures (for both 4h,7h,10h experiments).**

Compound layer does show an increasing trend with increasing time but it seems to reach saturation with increasing temperature. 500°C is said to be the limit temperature for the compound layer formation.

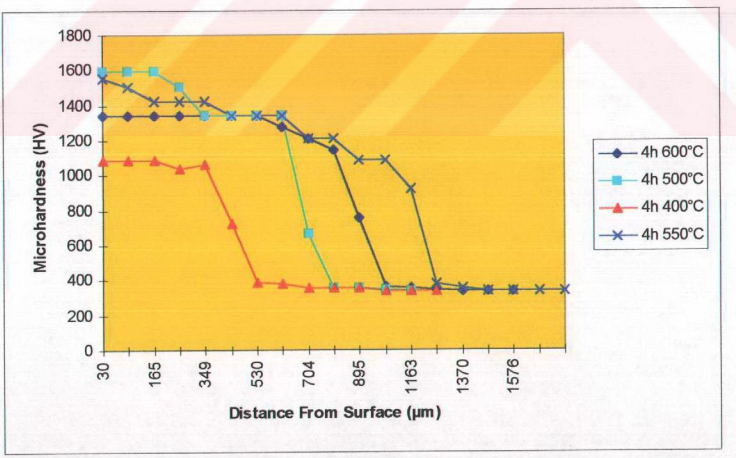


**Figure 5.12 The effect of process temperatures on the hardness behavior of the plasma nitrided samples treated at 4 hour.**

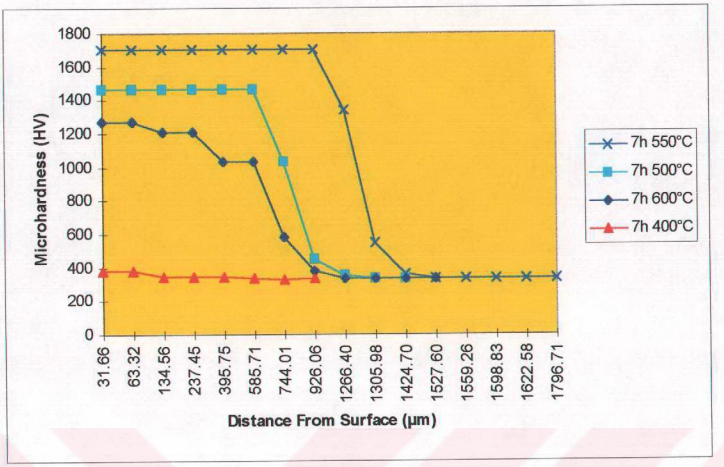


**Figure 5.13 The effect of process temperatures on the hardness behavior of the plasma nitrided samples treated at 7 hour.**

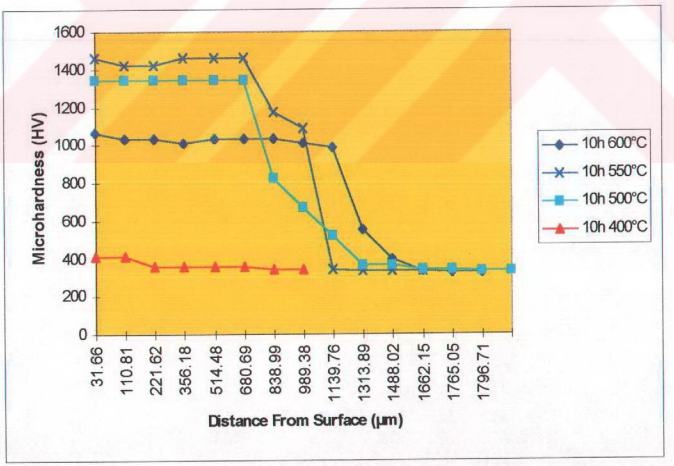


**Figure 5.14 The effect of process temperatures on the hardness behavior of the plasma nitrided samples treated at 10 hour.**

Typical hardness-depth profiles obtained for specimens treated in the temperature range 400-600°C are shown in Figure ( 5.12, 5.13 5.14). For a treatment temperature of 550°C the hardness in the nitrided region is increased from the bulk value 335 to 1699 HV, the maximum hardness value of all specimens. Surface hardness of the samples treated at the lowest temperature at 400°C (4 hour) is also quite high, but a dramatic increase in hardness is observed on specimens treated at 550°C (Figure5.9).

As seen in Figure 5.4 the process temperature has a strong influence on case depth . Both case depth and compound layer thickness increased greatly with increasing treatment temperature for the fixed treatment time of 4h due to an increased rate of nitrogen diffusion. The maximum compound layer thickness of all the samples investigated was measured on the sample treated at 7h 400°C.

Differences in the hardness of the layers are generally correlated to the size, shape and distribution of the nitride precipitates in the layer. At low temperatures, since the mobility of substitutional solutes is low, a growth limited situation prevails and leads to a low precipitate density and a consequent lower hardness of the layer.

Higher nitriding temperatures correspond to higher mobility of the substitutional solutes, but here a nucleation limited situation prevails. Therefore the precipitates are larger, again resulting in lower hardness. In addition, there is a tendency for the solubility of nitrides in the matrix to increase at higher temperatures. Thus in a qualitative way it is possible to consider the magnitude of hardness in the nitrided layer to be a function of temperature. With regard to the nitriding of AISI 316L stainless steel over a 7h period, a temperature of 550°C produces an optimum nitride precipitate size and density. Also, at higher temperatures the tempering effect may reduce the hardness of both the case and the core.

The effect of nitriding temperature on the hardness profiles, case depths, and compound layer thickness gives an indication of the kinetics of the reaction in the nitrided layer. As the plasma nitriding parameters such as pressure and gas composition are constant for the samples in question, temperature of the specimens were adjusted by adjusting the applied voltage.

Upon increasing the applied voltage, the amount of ionized gases and the kinetic energies of the ions increases. As a result, an increase in the current and in the temperature of the samples are observed as well.

By increasing the temperature, the rate of formation of FeN complexes and their redeposition on the surface is increased, leading to growth of the compound layer. Increasing process temperature increases the thickness of the diffusion layer (case depth) by increasing the rate of nitrogen diffusion through the layer.

An increase in the applied voltage has also the effect of increasing the amount of sputtering that a sample surface undergoes during the process. As a result of increasing voltage, i.e. process temperature, the amount of sputter cleaning taking place on the surface, which removes impurities such as oxide, increases. The enhanced removal of contaminants from the surface could increase its reactivity with nitrogen, thus allowing more nitrogen to react and producing thicker layers.

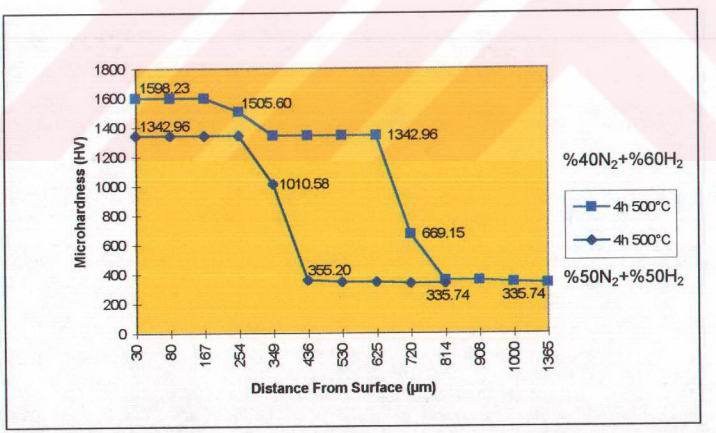


**Figure 5.15 Microhardness-depth profiles of samples plasma nitrided in atmospheres containing 40 and 50 vol.% $N_2$ at 500°C for 4h**

Nitrogen content of the plasma nitriding atmosphere seems to have significant influence on hardness-depth profiles of the samples (Fig.5.15). There does not seem to be any obvious correlation between $N_2$ content of the gas mixture and surface hardness levels. The case depths were similar for all the ratios of $N_2$ to $H_2$, but seems to slightly decrease as the amount of $N_2$ increases.

The increase in the compound layer thickness due to the increase of $N_2$ concentration in the nitriding atmosphere appears to be an effect of voltage. The voltage required to keep the workpieces at the process temperature were decreased with increasing $N_2$ concentration, which decreased the sputtering effect of the ions hitting the workpiece surface. But, as a contrary, compound layer thickness decreased with increasing $N_2$ concentration. On the other hand, higher sputtering effect prevents compound layer from growing on the samples treated in lower $N_2$ concentrations.

The slight decrease in case depth with increasing $N_2$ concentration can also be explained as an influence of the applied voltage. Decreasing nitrogen activity in the plasma due to the lower applied voltage may lead to increasing case depths.

**4.3 Wear Tests**

Pin-on-ring wear data of untreated and plasma nitrided specimens, tested under a load of 40N for a total sliding distance of 15000m, are summarized in Table 5.2. Plasma nitriding definitely reduced the wear rate of the material. The maximum improvement was achieved for the specimens at 550°C for 7 hours (7.550.40).

The changes in weight loss for the pins as a function of the sliding distance are shown in Figure 5.16 and Figure 5.17. The beneficial effect of treatment under the loading conditions employed in the present work is illustrated in this graph. It is evident that plasma nitriding substantially improves the wear performance of the steel and the degree of improvement depends on the plasma nitriding process conditions.

The improvements in the wear resistance can be related to mechanical properties rather than sliding properties of plasma nitrided samples. But in these present work

there does not make any experimental studies on the relation between the wear resistance and sliding properties (such as friction coefficient etc.)

**Table 5.2 Average weight loss values of wear specimens**

| AVERAGE WEIGHT LOSS (mgr) | | | | | | | | | | |
|---|---|---|---|---|---|---|---|---|---|---|
| | SLIDING DISTANCE (m) | | | | | | | | | |
| **GROUP** | **500** | **1000** | **1500** | **2000** | **3000** | **4000** | **5000** | **7000** | **10000** | **15000** |
| 1.400.40* | 15,5 | 8,8 | 12,5 | 14,7 | 28,1 | 38,2 | 51,4 | 104,6 | 171,3 | 284.9 |
| 1.500.40 | 1,3 | 1,1 | 4,3 | 3,7 | 4,9 | 17,6 | 16,6 | 42,5 | 142,2 | 373,5 |
| 4.400.40 | 31,7 | 30,5 | 32,6 | 34,3 | 77,6 | 68,1 | 64,3 | 118,5 | 220,3 | 328,2 |
| 7.400.40 | 4,2 | 10,3 | 14,1 | 11,9 | 44 | 51,1 | 61,8 | 117,7 | 183,1 | 321,7 |
| 10.400.40 | 4,1 | 21,2 | 21,5 | 22,5 | 96 | 59,2 | 65,3 | 146,3 | 207,8 | 358,2 |
| 4.500.40 | 15 | 19 | 24 | 69 | 105 | 103 | 89 | 151 | 311 | 378 |
| 4.500.50 | 13,5 | 26,5 | 59 | 80 | 129 | 80 | 90 | 266 | 375 | 430 |
| 7.500.40 | 7,9 | 4,5 | 1,5 | 0,7 | 19,6 | 39,8 | 60,3 | 129,7 | 250,1 | 360,5 |
| 10.500.50 | 2 | 5 | 2 | 1,5 | 1,4 | 4,9 | 6,4 | 5,3 | 8 | 14,4 |
| 4.550.40 | 2 | 2 | 1,2 | 2,8 | 2 | 1,7 | 1 | 4,8 | 10 | 18,9 |
| 7.550.40 | 1,6 | 0,6 | 0,9 | 0,8 | 1 | 1 | 1 | 2 | 5,5 | 7,3 |
| 10.550.50 | 1,9 | 2,7 | 1 | 1,3 | 1,8 | 5,9 | 3 | 4,1 | 12,1 | 16,2 |
| 4.600.40 | 0,4 | 0,2 | 0,7 | 0,4 | 0,4 | 2,5 | 2,9 | 3,3 | 8,1 | 13,7 |
| 7.600.50 | 0,7 | 0,7 | 1,3 | 1 | 0,7 | 1,6 | 2,5 | 3,1 | 7,2 | 18,8 |
| 10.600.40 | 3,7 | 8 | 5 | 9 | 4,4 | 5,1 | 2,9 | 3,6 | 3,3 | 10 |
| Untreated | 46,4 | 45,3 | 59,6 | 69,1 | 114 | 130 | 137 | 270,3 | 505,2 | 637,6 |

(* see table 4.3 for the process conditions of the groups)

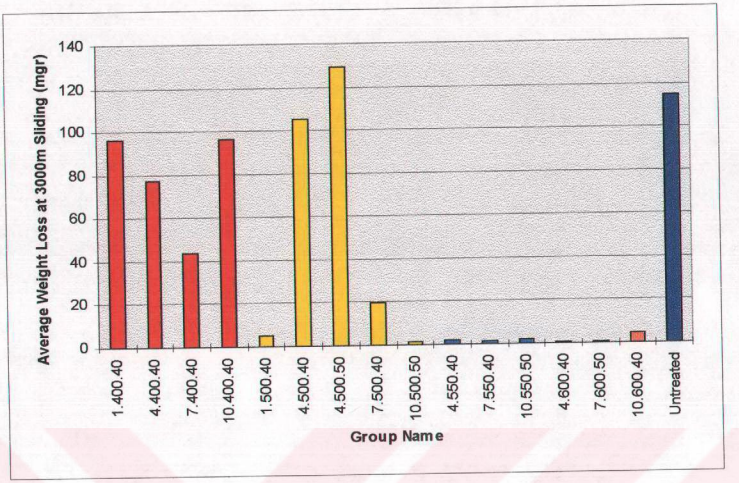


**Figure 5. 16 Wear rates as a function of average weight loss at 3000m dry sliding conditions for all of the specimen groups.**

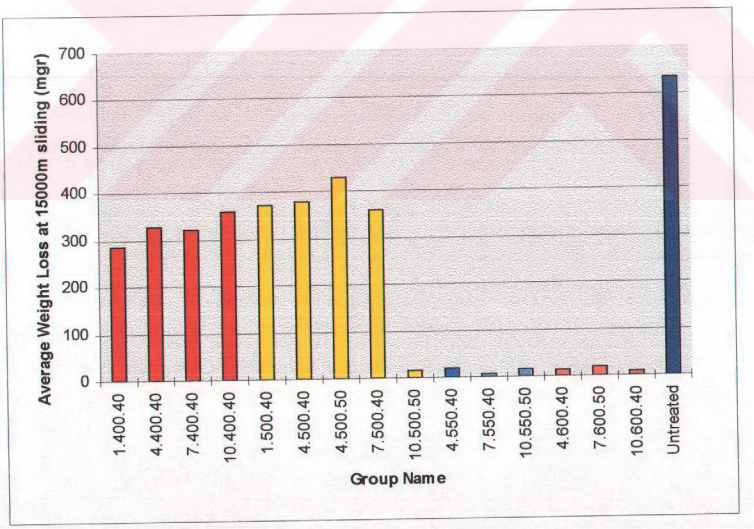


**Figure 5. 17 Wear rates as a function of average weight loss at 15000m dry sliding conditions for all of the specimen groups.**

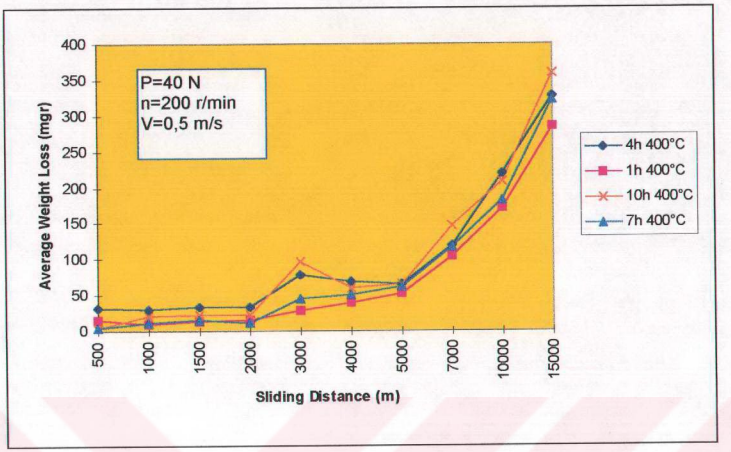


**Figure 5.18 The effect of treatment time on the average weight loss (wear rate) of the plasma nitrided samples treated at 400°C**

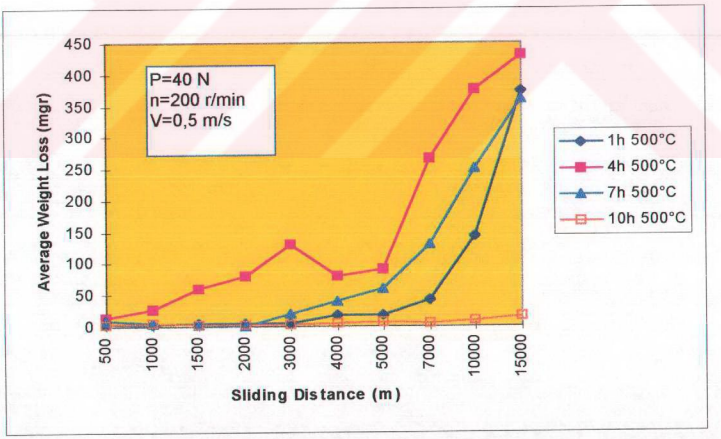


**Figure 5. 19The effect of treatment time on the average weight loss (wear rate) of the plasma nitrided samples treated at 500°C**

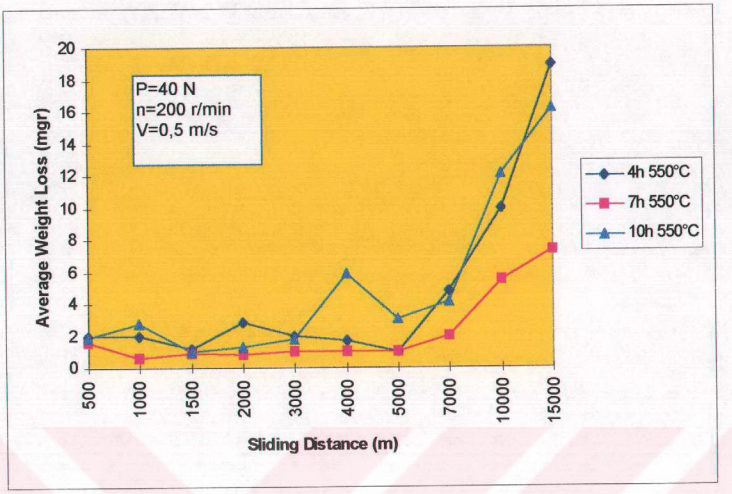


**Figure 5. 20 The effect of treatment time on the average weight loss (wear rate) of the plasma nitrided samples treated at 550°C**

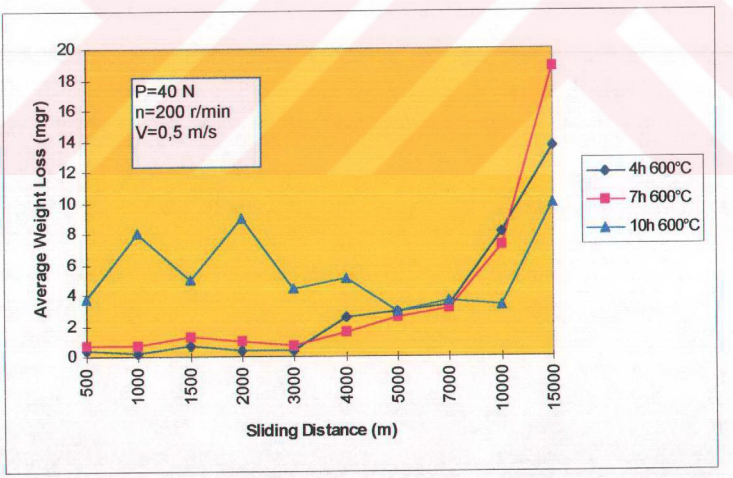


**Figure 5. 21 The effect of treatment time on the average weight loss (wear rate) of the plasma nitrided samples treated at 600°C**

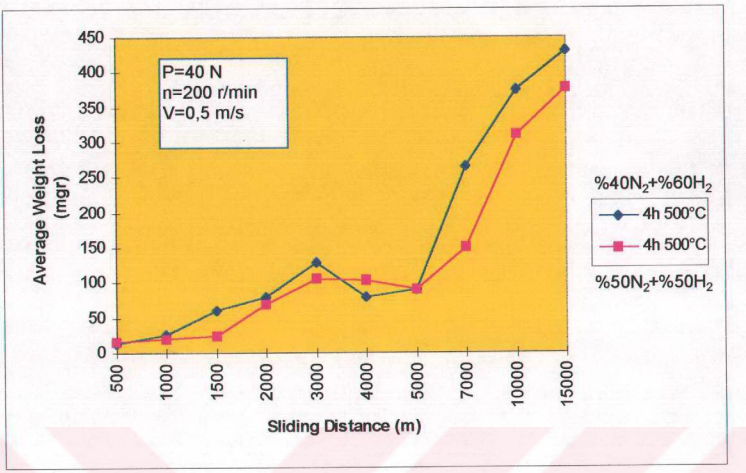


**Figure 5.22 The effect of gas compositions on the wear rate of the plasma nitrided samples treated at 4 hour 500°C**

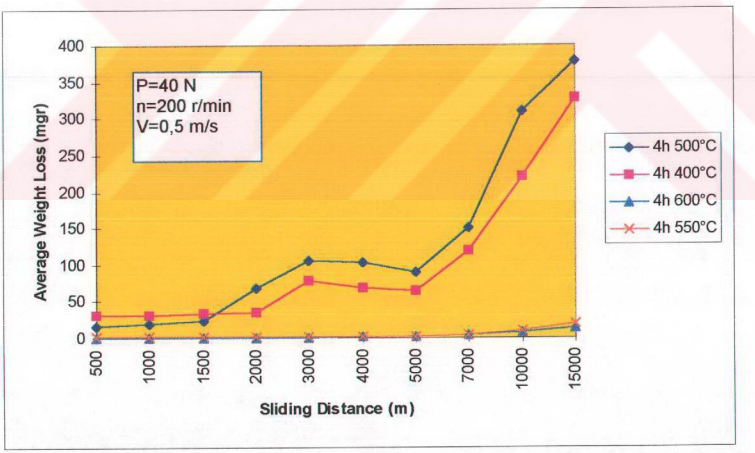


**Figure 5.23 The effect of treatment temperatures on the average weight loss (wear rate) of the plasma nitrided samples treated at 4 hour.**

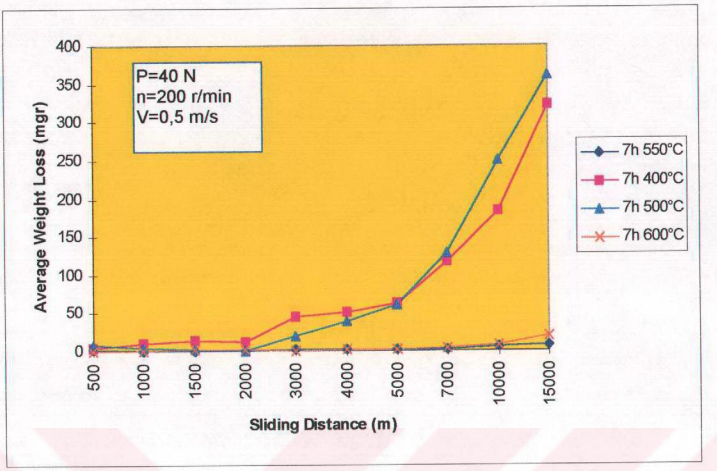


**Figure 5.24 The effect of treatment temperatures on the average weight loss (wear rate) of the plasma nitrided samples treated at 7 hour.**

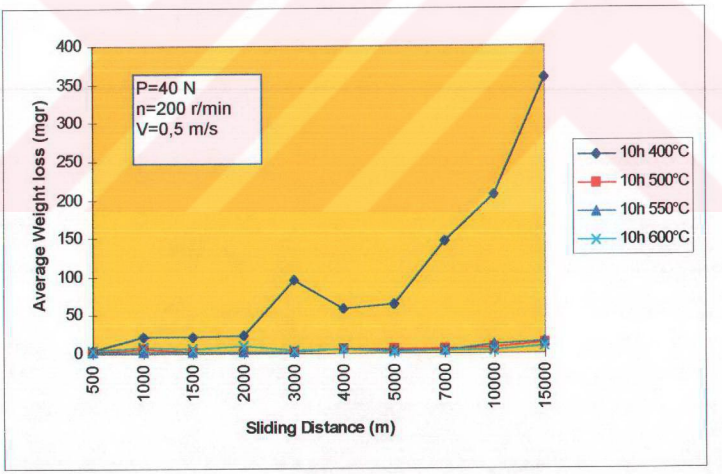


**Figure 5.25 The effect of treatment temperatures on the average weight loss (wear rate) of the plasma nitrided samples treated at 10 hour**

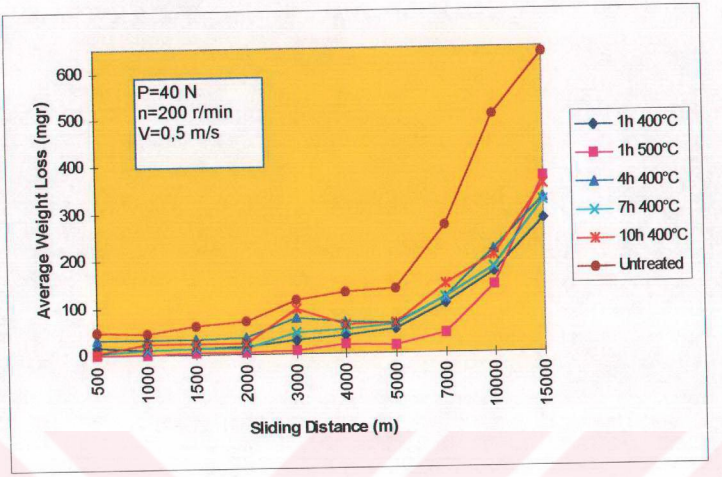


**Figure 5. 26 Average weight loss of untreated and plasma nitrided specimens.**

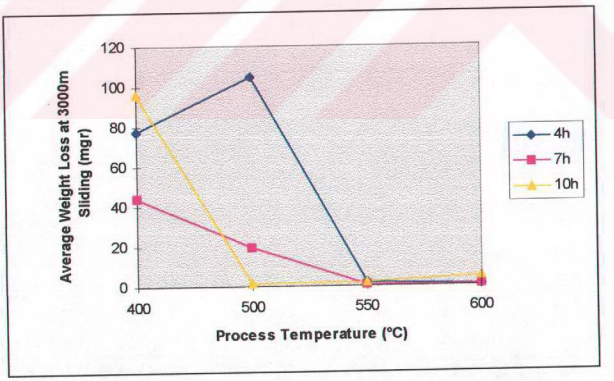


**Figure 5.27 Average Weight Loss changes as a function of plasma nitriding temperatures (for both 4h,7h,10h experiments) at 3000m sliding.**

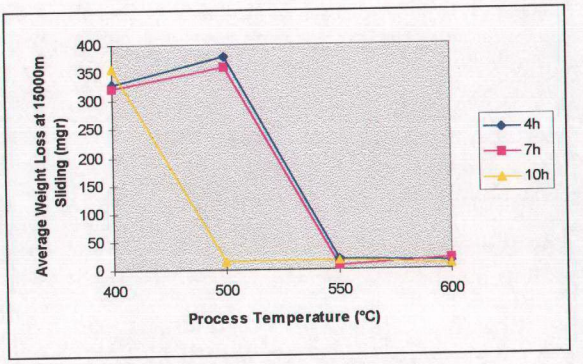


**Figure 5.28 Average Weight Loss changes as a function of plasma nitriding times (for both 400, 500, 550 and 600°C experiments) at 15000m sliding.**

Among the treated groups, it can be seen that initial wear rate (after 15000m sliding) was greatest for specimens plasma nitrided at 500°C (10.500.50), which has no compound layer and a relatively highest hardness. On the other hand, total wear rate (after 3000m sliding) is greatest for specimens treated for 4h (4.500.50) which has the lowest hardness and minimum case depth values of all plasma nitrided groups.

Under the test conditions, untreated steel behaved poorly in terms of dry wear resistance due to its low hardness. Worn surfaces of untreated specimens revealed severe running-in wear at the beginning of the test. As a result, metallic wear debris and material loss were observed. The weight loss of untreated specimens increased almost linearly with increasing sliding distance, and always remained higher than those of the plasma nitrided samples (Figure 5.17).

Severe running-in wear did not occur in the plasma nitrided specimens and wear proceeded in a mild mode throughout the test.

Worn surfaces of untreated and some plasma nitrided samples after a sliding distance of 15000m is shown in Fig.5.29. The wear scars formed on the pins are parallel to the rolling direction of the wear rings. Examination of the untreated

samples at the early stage of testing revealed extensive wear by adhesion with local fusion, i.e. severe adhesive wear. On the other hand, plasma nitrided samples are seen to be lightly scored with some abrasive particles which are obviously the fragments of compound layers broken at the very outset of the wear test during asperity deformation.

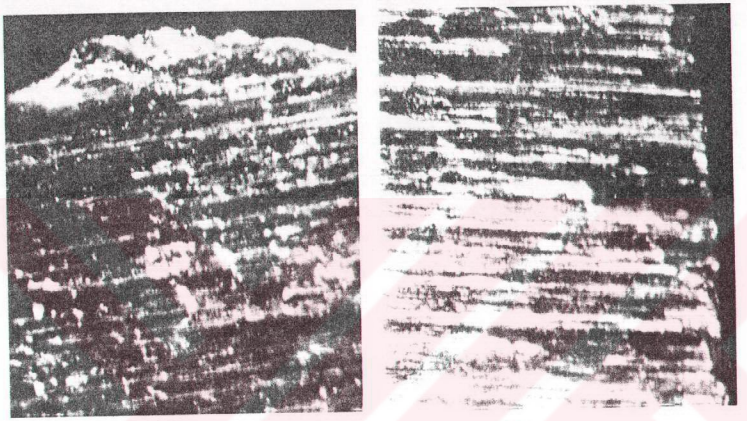

a b

**Figure 5.29 Worn Surface photographs of untreated a) and 1.500.40 nitrided b) specimens after 15000m dry sliding tests**

Wear surfaces of an untreated and a (1.500.40) plasma nitrided samples that had covered, under test, a sliding distance of 15000m are shown in Figure 5.29. A considerable extent of plastic deformation was observed on the wear surface of the untreated specimen . The surface is rough and deeply torn typical of the severe wear. The plasma nitrided sample which exhibited many shallow grooves experienced a reduced degree of damage and plastic deformation on the wear surface. The worn surface of plasma nitrided sample showed typical properties of mild wear with smooth appearance in comparison with the untreated sample.

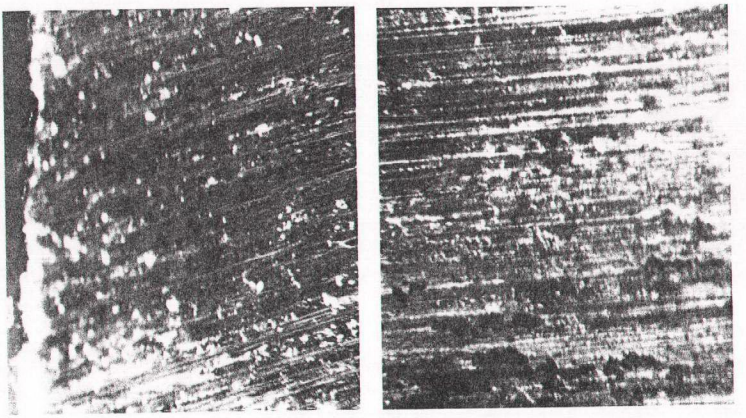

a b

**Figure 5.30 Optical microscope photographs showing the wear surfaces of a) 4.500.40 and b) 7.550.40 nitrided samples after a sliding distance of 15000m**

Optical microscopy examinations show that the worn surface and debris morphology are in close relationship with the wear mechanism. Optical micrographs of wear debris of some specimens are given in Figure 5.30. Large and predominantly metallic debris of untreated sample (Figure 5.29a ) shows that, the specimen severely worn under the test conditions. The oxidized appearance of the worn surface and the generation of oxide wear debris indicate that mild oxidative wear was dominant in the wear of the nitrided samples.

The higher weight loss of sample 10.400.40 especially at the first stage of the test (3000m) seems to be an effect of its relatively thick compound layer (15.84μm) and low hardness (See Table 5.1 ). Here, thicker compound layer increases the wear rate of the sample by breaking off and by forming abrasive particles. The particles generated from breakdown of the thicker compound layers change the wear mechanism from adhesive to abrasive. Thus the wear rate is increased with increasing compound layer thickness.

There is very little difference among the wear rates of samples within the first 3000m of dry sliding, except 7.500.40 samples. The weight loss values of samples

differs with increasing sliding distance. Thus, properties of the nitrided layers, i.e. plasma nitriding parameters affect the wear resistance of the samples. Higher values of process temperature and lower surface hardness, and shorter process times leading to lower hardness values, seems to be the main reason of low wear resistance observed on samples 1.500.40 and 7.500.40.

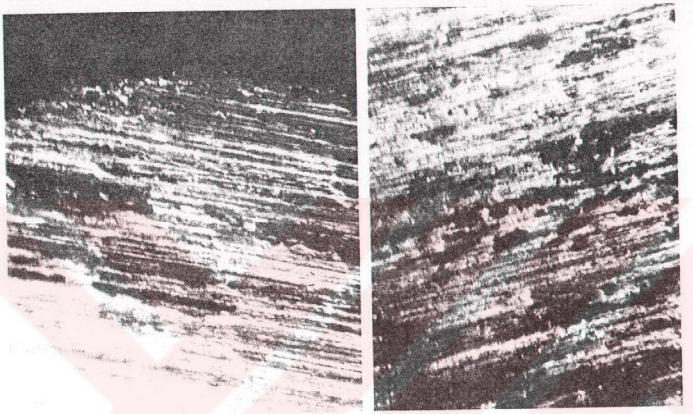

a b

**Figure 5.31 Worn Surfaces of 7.600.50 and 10.600.40 plasma nitrided specimens after 15000m dry sliding tests**

It can be seen that the weight loss increased with test time (compare with Figure 5.16 and Figure 5.17 ). The hardness of the surface is the most effective factor with respect to wear rate. Under the same conditions, the minimum weight loss is observed on the samples treated at 550°C for 7h due to its high hardness value, i.e. 1699HV (see Fig.5.28 ). The reason for the rapid weight loss of samples treated at 400°C is also related to its relatively low hardness of the case which is not strong enough to support the thick and brittle compound layer.

When the material loss is compared on the basis of the test results, it is found that the combination of high hardness, thin compound layer and thick case is better in reducing the material loss under the test conditions.

# CHAPTER SIX
# CONCLUSIONS

## 6.1 CONCLUSIONS

The main conclusions obtained in this study about effects of plasma nitriding process parameters on mechanical and structural characteristics of austenitic AISI 316L stainless steel, can be summarized as follows:

- Hardness level, case depth, and compound layer thickness are strongly affected by the process time.
- With regard to the process time, the sample plasma nitriding over a period of 7h (at 550°C) produces an optimum nitride precipitate size and density leading to the maximum surface hardness.
- For the shortest time (1h) the nitrogen uptake and precipitate density are low and therefore the amount of hardening is also low. Over extended nitriding periods, surface hardness of samples decreased due to the coarser precipitates. For example,10h nitriding processes have lower surface hardness aganist 4 or 7h nitriding processes at the same temperature).
- The case depth and compound layer thickness are change parabolic with time. Compound layer thickness shows an increasing trend with increasing time, but it seems to reach a saturation. The saturation may be explained by surface sputtering which causes decarburisation of the surface leading to tranformation of iron-nitrides from $\varepsilon$ to $\gamma'$. This transformation has a limiting effect on compound layer thickness.

- The process temperature has a strong influence on both case depth and compound layer thickness. Diffusion layer thickness increase greatly with increasing treatment temperature. Beside the process temperature, volumetric ratio of $N_2$ is the other effective parameter in determining the compound layer thickness. From our experiments we found that 40% $N_2$ volumetric ratio is the saturation value for compound layer formation.
- At low temperatures (400°C), since the mobility of substitutional solutes is low, a growth limited situation prevails and leads to a low precipitate density and a consequent lower hardness of the layer. Higher nitriding temperatures (550°C) correspond to higher mobilities of the substitutional solutes, but here a nucleation limited situation prevails. Therefore the precipitates are larger, again resulting in lower hardness (in 600°C experiments).
- There does not seem to be any obvious correlation between $N_2$ content of the gas mixture and surface hardness levels. The case depths are similar for all the ratios of $N_2$ to $H_2$, but seems to slightly decrease as the amount of $N_2$ increases.
- It is evident that the wear resistance of the steel is increased markedly by plasma nitriding. The degree of improvement depends on the plasma nitriding process conditions.
- The maximum wear resistance was achieved for the specimens plasma nitrided at 550°C for 7 hours due to its high hardness value. Thus, the hardness of the surface is a very important factor with respect to wear rate.
- Higher values of process temperature, which leads to relatively lower surface hardness, and shorter process times leading to lower hardness values, have been determined as the main causes of relatively low wear resistance of some samples.
- When the material loss is compared on the basis of the test results, it is found that the combination of high hardness, thin compound layer and thick case is better in reducing the extent of material loss under the test conditions.

# REFERENCES

Albarran, J.L., Juarez-Islas, J.A., & Martimez, L. (1992). Nitride width and microhardness in H-12 ion nitrided steel. Materials Letters, 15, 68-72.

Aksakallı, H. (1198). Fatigue Properties of Surgical Implant Materials, (M.Sc. Thesis). İzmir, Graduate School of Natural and Applied Science of Dokuz Eylül University.

American Society for Testing and Materials. (1982). a) E 466-76 and b) E 739-80. AnnualBook of ASTM Standards, part 10. Philadelphia.

Avner, S.H., (1974) Introduction to Physical Metallurgy , pp. 362-375.

Bell, T., & Sun, Y. (1990). Load bearing capacity of plasma nitrided steel under rolling-sliding contact. Surface Engineering, 6 (2), 133-139.

Berghaus, B. (1932). Process for the surface treatment of metal pieces (German). German patent DRP 668.639.

Berghaus, B. (1939). Vacuum furnace heated by a glow discharge (German).German patent DRP851.540.

Berghaus, B. (1956). Control of glow discharge processes. US patent 3.018.409.

Berghaus, B. (1961). Method and apparatus for controlling glow discharge processes. US patent3.345.280.

Chyou, S.D., & Shih, H.C. (1990). Structure and electrochemical properties of plasma-nitrided low alloy steel. Materials Science and Engineering, A129, 109-117.

Cohen, A., Boas, M., & Rosen, A. (1986). The influence of ion nitriding parameters on the hardness layer of 15-5 ph stainless steel. Thin Solid Films, 141, 53-58.

Collins, J.A. (1981).Failure of Materials in Mechanical Design p.369 John Wiley & Sons.

Çelik, A., & Karadeniz, S. (1995). Improvement of the fatigue strength of AISI 4140 steel by an ion-nitriding process. Surface & Coatings Technology, 72, 169-173.

Çelik, A., & Karadeniz, S. (1996). Investigation of the compound layer formed during ion nitriding of AISI 4140 steel. Surface & Coatings Technology, 80, 283-286.

Edenhofer, B. (1974 a). Physical and metallurgical aspects of ionitriding-part1. Heat Treatment of Metals, 1, 23-28

Edenhofer, B. (1974 b). Physical and metallurgical aspects of ionitriding-part2. Heat Treatment of Metals, 2, 59-67.

Edenhofer, B. (1976). The ionitriding process-thermochemical treatment of steel and cast iron materials. The Metallurgist and Materials Technologist, 8, 421-426.

Haruman, E., Bell, T., & Sun, Y. (1992). Compound layer characteristics resulting from plasma nitrocarburising in atmospheres containing carbon dioxide gas additions. Surface Engineering, 8 (no:4), 275-282.

Hombeck, F., & Bell, T. (1991). Environmentally harmless plasma thermochemical processes. Surface Engineering, 7 (1). 45-52.

Hudis, M. (1973). Study of ion-nitriding. Journal of Applied Physics, 44, 1489-1496.

İnal, O.T., & Robino, C.V. (1982). Structural characterisation of some ion-nitrided steels. Thin Solid Films, 95, 195-207.

Jones, J.K., & Martin, S.W. (1964). Brazing Glow Discharge. Metal Progress, 95-98.

Jones, B.K., & Martin, J.W. (1977). Residual stress distribution in nitrided En 41B steel as function of case depth. Metals Technology, 4, 520-523.

Karadeniz,S.,& Günay,H. (1999). Experimental investigation of the hardening ability of a plasma nitrided AISI 304 stainless steel. Mamtek 99

Karamış, M.B. (1991). Friction and wear behavior of plasma nitrided layers on 3% Cr-Mo steel. Thin Solid Films, 203, 49-60.

Karamış, M.B. (1992). Some effects of the plasma nitriding process on layer properties. Thin Solid Films, 217, 38-47.

Karamış, M.B. (1993). Wear properties of steel plasma nitrided at high temperatures. Materials Science and Engineering, A168, 49-53.

Karoğlu, S. (1998). Plasma Nitriding behavior of AISI 5140 Steel, (Ph.D. Thesis). İzmir, Graduate School of Natural and Applied Science of Dokuz Eylül University.

Kovacs, W., & Russelll, W. (1986). Proc. Int. Conf. on Ion Nitriding. T. Spalvins (Ed.), An introduction to ion nitriding. (pp. 9-16). ASM International.

Kölbel, J. (1965). The formation of nitride layers in glow discharge nitriding. (German).Report 1555, Forschung Bericht Lande Nordrhein-Westfalen.

Kuppusami, P., Sundararaman, D., & Raghunathan, V.S. (1993). Comparative study of plasma nitriding behavior of a type 316 stainless steel and a microalloyed steel. Surface Engineering, 9 (2). 137-141.

Kurny, A.S.W., Mallya, R.M. & Mohan Rao, M. (1986). A study on the nature of the compound layer formed during the ion nitriding of En40B steel. Materials Science and Engineering, 78, 95-100.

Kurny, A.S.W., Mallya, R.M., & Mohan Rao, M. (1988). On the formation of austenite during ion-nitriding of armco iron. Journal of the Less-Common Metals, 144, 201-207

Lampe, T., Eisenberg, S., & Laudien, G. (1993). Compound layer formation during plasma nitriding and plasma nitrocarburising. Surface Engineering, 9 (1), 69-76.

Li, S., Manory, R.R. (1996). Surface morphology and compound layer pores of plasma nitrocarburised low carbon steel. Metallurgical and Materials Transsactions A, 27A, 135-143.

Michalski, J. (1993). Ion nitriding of Armco iron in various glow discharge regions. Surface and Coatings Technology, 59, 321-324.

Miyamura, H., Takada,J., Kuwahara,H., & Kikuchi, S. (1986). Ion-nitriding behaviour of Fe-Ti alloys in the $\alpha$-phase region. Journal of Materials Science, 21, 2514-2518.

Özbaysal, K., İnal, O.T., & Romig, A.D. (1986). Ion-nitriding behaviour of several tool steels. . Materials Science and Engineering, 78, 179-191.

Parr J., & Hansan A., (1965), An Introduction to Stainless Steels , pp. 52-63

Peng, Q.F. (1989). Improving abrasion wear by surface treatment. Wear, 195-203.

Phillips, V.A., & Seybolt, A.U. (1968). A Transmission electron microscopic study of some ion-nitrided binary iron alloys and steels. Transactions of the Metalurgical Society of AIME, 242, 2415-2422.

Rembges, W. (1986). Proc. Int. Conf. on Ion Nitriding. T. Spalvins (Ed.), Fundamentals applications and economical considerations of plasma nitriding. (pp. 189-198). ASM International.

Robino, C.V. & İnal, O.T. (1983). Ion nitriding behavior of several low alloy steels. Materials Science and Engineering, 59, 79-90.

Sato, K., Takahashi, K., Inoue, Y., Yamazaki, T., & Nitoh, Y. (1988). Surface layers produced by ion nitriding of austenitic Fe-Mn-Al alloys and the effects on hardness and corrosion resistance. Journal of Materials Science, 23, 4445-4449.

Seybolt, A.U. (1969). Some observations on the metallurgy of ion-nitriding. Transactions of the Metalurgical Society of AIME, 245, 769-778.

Sun, Y., & Bell, T. (1991). Plasma surface engineering of low alloy steel. Materials Science and Engineering, A140, 419-434.

Sun, Y., Bell, T., & Wood, G. (1994). Wear behavior of plasma nitrided martensitic stainless steel. Wear, 178, 131-138.

Sharma, S.C., Satish, B.M., (1998). Dry sliding wear of short glass fibre reinforced zinc-aluminium composites. Tribology International , 31, 183-188.

Takada, J., Ohizumi, Y., Miyamura, H., Kuwahara, H.,Kikuchi, S., & Tamura, I. (1986). Ion-nitriding of an Fe-19wt% Cr alloy. Journal of Materials Science, 21, 2493-2496.

Tibbetts, G.G. (1974). Role of nitrogen atoms in ion-nitriding. Journal of Applied Physics, 45, 5072-5073.

Zlatanovic, M., Kunosic, A., & Tomcik, B. (1986). Proc. Int. Conf. on Ion Nitriding. T. Spalvins (Ed.), New development in anode plasma nitriding. (pp. 47-51). ASM International.